

Final Report

# Interaction of Shock Wave and Boundary Layers at Hypersonic Speeds

(NASA-CR-4274) FLOW SEPARATION IN SHOCK  
WAVE BOUNDARY LAYER INTERACTIONS AT  
HYPERSONIC SPEEDS Final Report (George  
Washington Univ.) 45 p

CSCL 01A

H1/07

Unclas  
0257036



NASA Contractor Report 4274

# Flow Separation in Shock Wave Boundary Layer Interactions at Hypersonic Speeds

A. Hamed

*The George Washington University  
Joint Institute for Advancement of Flight Sciences  
Langley Research Center  
Hampton, Virginia*

Prepared for  
Langley Research Center  
under Contract NAS1-18458



National Aeronautics and  
Space Administration  
Office of Management  
Scientific and Technical  
Information Division

1990



## INTRODUCTION

Shock boundary layer interactions are usually the cause of flow separation at hypersonic and supersonic speeds. In addition to increasing the drag and the aerodynamic heating on the aircrafts and missiles, they adversely affect the inlet and control surface performance. The conditions leading to flow separation and the subsequent changes in the flow have been the subject of extensive research efforts over the past 30 years. The results of these investigations have been compiled and discussed in several excellent reviews [1-4]. However, in spite of these efforts, the combined influence of viscous-inviscid interactions, turbulence, and compressibility on the resulting complex flow fields is not fully understood at high speeds. Owen [5] discussed the problems associated with the experimental measurements of flows at hypersonic speeds, and the inadequacy of existing experimental techniques in shock boundary interactions involving separation, time dependent flow reversal, and high levels of turbulence.

The focus of the present work is the assessment of the experimental data on separated flow in shock wave turbulent boundary layer interactions at hypersonic speeds. The data base will consist mainly of two dimensional and axisymmetric interactions of shock wave and turbulent boundary layer. Only two configurations will be considered, namely compression corner or cylinder-flare, and externally generated oblique shock interactions with boundary layers over flat plates or cylindrical surfaces. Interactions in forward or backward steps will not be included. This choice is based on the absence of any characteristic length, with the exception of the incoming boundary layer thickness, in the two configurations shown in Fig. 1.

This work was supported under NASA Contract NAS1-18458, Task 19, by the Theoretical Flow Physics Branch, Fluid Mechanics Division, with The George Washington University.

### INCIPIENT SEPARATION

The conditions for incipient separation due to shock boundary layer interactions in two dimensional hypersonic flow have been determined experimentally by a number of investigators [6-11]. The Mach number in these experiments ranged between 6 and 13 and the Reynolds number based on the boundary layer thickness before the interaction was in the range of  $10^5$ - $10^6$ . The results indicated that the resistance to separation increased with the Mach number and decreased with the Reynolds number [7-11]. Since the boundary layer thickness on a full scale model is usually much larger than that on a smaller wind tunnel model, the effect of the Reynolds number on the shock boundary layer interactions and flow separation need to be understood, if the experimental data is to be used in practical applications. For this reason, incipient separation data for supersonic two-dimensional flow [12-18] is included in the present survey, since it covers a wider range of Reynolds number [ $10^4 < Re_\delta < 10^7$ ].

The experimentally determined [6-20] incipient separation conditions in hypersonic and supersonic flows are presented in Fig. 2. One can see the variation in the incipient separation angle in a compression corner with the Reynolds number for different values of Mach number. The Reynolds number in the figure is based on free stream conditions and the incoming boundary layer thickness before the interaction. Such a plot was first used by Kuehn [12] to present his experimental results and later appeared in other references, with a continuously expanding incipient separation data base. Some of the incipient separation data in Fig. 2 were obtained in the interaction of an impinging externally generated oblique shock with the turbulent boundary layer on a flat plate. In these cases, an equivalent

angle is defined which would produce the same overall pressure ratio. Holden [6, 10], Kuehn [12] and Settles et al. [18] demonstrated the equivalence between the separation data in the compression corner and this configuration, when correlated in terms of the overall pressure ratio across the incident and reflected shock.

#### Effect of Mach Number

The incipient separation angle increased with the Mach number for both supersonic and hypersonic flows. This influence decreases however with increasing Mach number and is very weak in hypersonic flow above Mach eight.

#### Effect of Reynolds Number

Kuehn [12] conducted one of the earliest experimental investigations to study the Mach and Reynolds number effects on incipient separation in shock wave turbulent boundary layer interactions. His results indicated that the flow resistance to separation increased with the Mach number ( $2 < M < 4$ ) and decreased with the Reynolds number. The supersonic data reported earlier by Drougge [13] and later by Sterrett and Emery [14] and by Kessler [15] exhibited the same Mach and Reynolds number effects on incipient flow separation. The experimental results of Roshko and Thomke [16] over a range of Reynolds number which was at least an order of magnitude higher, showed a trend reversal with a moderate increase in the resistance to separation with  $Re$ , but the Mach number effect did not change. An increase in the boundary layer resistance to separation with the Reynolds number was also reported by Law [17] for  $M = 2.96$ . Settles et al. [18] presented incipient separation results in which the incipient separation angle was practically independent of the Reynolds number.

Different explanations have been advanced to explain the difference in the Reynolds number trends in the experimentally measured transition.

Elfstrom [7] related the trend reversal of the Reynolds number to the changes in the wake component of the boundary layer, and was able to predict it analytically using a simple two-layer model. Holden [3] offered another explanation based on the non-equilibrium development of the turbulent boundary layers in some of the experiments. Bushnell et al. [19] demonstrated that the nonequilibrium effects due to the favorable pressure gradient on the tunnel walls can persist at distances up to one hundred times the boundary layer thickness downstream of the nozzle exit. Roshko and Thomke [16] and Settles et al. [18] however, reported the same incipient separation trends with the Reynolds number on tunnel walls and on axisymmetric models, which contradicts the argument that the tunnel wall boundary layers are fuller [20, 21] and therefore harder to separate. Bushnell et al. [19] demonstrated also that downstream of transition, the turbulent boundary layer velocity profile power exponent  $N$  first decreases until the boundary layer becomes fully developed, then increases with the Reynolds number as shown in Fig. 3. Based on this, Hankey and Holden [3] explained that Kuehn's measurements were obtained in the range where as a result of boundary layer relaxation, the profiles became less full, hence the decrease in resistance to separation with the Reynolds number. The Roshko and Thomke [16] data on the other hand were in the range where  $N$  increased with  $Re_\delta$ . Holden also explained the trend reversal between the experimental measurements reported in two of his studies [6, 10] in terms of the effect of nonequilibrium on the skin friction variation with the Reynolds number. Holden [10] also pointed out the difficulty of attempting to induce transition prematurely in hypersonic flows. He mentioned the possibility of a transitional rather than a fully turbulent boundary layer



in the interaction zone when the boundary layer was tripped as in Kuehn's experiments.

#### Effect of Surface Cooling

All of the hypersonic incipient separation experiments [6-10] with the exception of reference 11, involved surface cooling. The experimental results of Holden [10] and Elfstrom [7] indicate that cooling increases the boundary layer resistance to separation at hypersonic speeds. Favorable effects of wall cooling on both the incipient separation angle and separation length were also measured in supersonic flows by Spaid and Frishett [26] and Gulbran et al. [20]. A nearly linear trend of increasing incipient separation angle with decreasing wall temperature was reported by Spaid and Frishett [26].

#### End Effects

Few of the surveyed experiments used fences to reduce end effects, but only Holden [6, 10] verified the diminished end effects on the measurement at the center through varying the model width in the absence of fences. According to experimental evidence, very moderate bleeding (2-4% of the boundary layer, mass flow) can control flow separation in shock boundary layer interaction. Delery [2] discussed this phenomena and explained the cause for the strong influence of removing a small amount of the flow in the separation zone on controlling separation. The end effects might therefore play a significant role in flow separation. Coleman and Stollery [22], Kuehn [23] and Rose et al. [24] obtained incipient separation data in axisymmetric configurations. Coleman and Stollery [22] obtained incipient separation data in a cylinder-flare axisymmetric configuration to assess the end effects in their compression corner incipient separation results [8]. They determined that the incipient separation angles differed only by one

degree in a cylinder-flare model from the equivalent wedge compression corner at  $M=9$ . The surface pressure distributions near the corner were also identical in the two geometries under the same flow condition. Their results are shown in Fig. 4 together with Kuehn's data [12,23] which exhibit larger differences between the axisymmetric and two dimensional data at  $M=2.4$ .

#### Incipient Separation Detection Methods

Several methods have been used by the different investigators to identify the conditions for incipient separation in shock wave turbulent boundary layer interactions. The experimentally measured surface pressures [7,9,12-14,16-18,23-24], temperatures [8], and skin friction [6,10] have been used in conjunction with different criteria to detect flow separation. Incipient separation conditions have also been deduced from shadowgraphs and schlieren [7-10,25,26] pictures as well as from surface oil flow visualization [17] and powder deposition techniques [26]. Law [17], Apples and Richards [25] and Spaid and Frishett [26] determined the incipient separation conditions in their experiments using different methods, and demonstrated that experimentally determined incipient separation angles in a compression corner can be dependent on the method of detection.

Different criteria have been used in detecting separation from the surface pressure measurements. Kuehn [12] identified separation with the appearance of three inflection points in the measured surface pressure distribution in the compression corner experiments. Coleman and Stollery [8] and Drougge [13] also used the first appearance of a kink in the surface pressure distribution as the criterion for incipient separation. This criterion is not suitable in the case of externally generated incident

shock, since Green [27] found that this change in the pressure distribution occurred only when a relatively large separation region was formed.

Another separation criterion is based on the variation of the measured surface pressure near the corner with the corner angle. This criterion was used by Roshko and Thomke [16] and by Elfstrom [7] who identified separation angle with the inflection in the pressure versus corner angle plot. The disappearance of the overshoots in the surface pressure distribution was suggested by Elfstrom [7] as a criterion for incipient separation in hypersonic flows.

Coleman and Stollery [8] used the measured surface heat transfer distributions to detect separation in their experiments. They identified the separation angle with the conditions when the heat transfer rate started to increase just ahead of the hinge line of the compression corner. Experimental evidence of this increase in the heat transfer were also reported by other investigators including Holden [10], Holloway et al. [28] and Gadd et al. [29].

Due to the unsteady characteristics in the separation zone, Holden [6, 10] used the surface shear measurements instead of pressure, to detect separation. Incipient separation was identified with the condition where the time average of surface shear was zero at one point. This approach has not been used by many other investigators because of the difficulties associated with the accurate measurement of the extremely small wall shear stress values near separation.

Shadowgraph and schlieren pictures have been used to detect separation due to shock turbulent boundary layer interactions in supersonic and hypersonic flows. The change in the shock wave angle in the schlieren picture due to the formation of a double shock system was used by Drougge

[13] and Sterrett and Emery [14] as the criteria for incipient separation in a compression corner. Another method which was extensively used by a number of investigators [7-10,25,26] was based on measuring the separation length from the schlieren pictures. The separation length has also been determined from the surface pressure distribution, in which case the separation and reattachment points are identified with the first and third inflection points.

Surface oil flow visualization has also been used to detect flow separation [25,26]. In this method the liquid is applied to the surface before the test and the flow separation is identified by the liquid line where the oil has accumulated. Because the liquid line thickness is comparable to that of the separation bubble, the effect of their interaction can be a source of error. Apples and Richards [25] studied this phenomena by running some of the tests for much larger times, in which case the accumulated oil was entrained into the separation region and filled the separation bubble. In order not to disturb the separation bubble for a small separated region, the same authors demonstrated that the interaction can be minimized by applying a very small quantity of oil ahead of the expected separation region. They also used high speed schlieren pictures to study the effect of the flow unsteadiness in the separated regions which was negligible in their experiment. Since liquid accumulation can also result from the balance between the wind and buoyancy forces, Spaid and Frishett [26] used a powder deposition technique to verify their oil flow results. The two methods were in agreement within the liquid line reading uncertainty.

In principle, the distance  $L_s$  between the separation and reattachment points is measured at different shock strengths. Plots of the measured

separation length verses the corner angle are then used to extrapolate the angle of incipient separation  $\alpha_I$ , corresponding to  $L_s = 0$ . Coleman and Stollary [8] based their results on a linear interpolation, while others [17,25] used more than two separation data points for their extrapolation. One source of error in this detection method is the uncertainty in locating the separation point from the schlieren photographs. By including measurements for small separations with  $L_s/\delta < 5.0$ , Apples and Richards [25] demonstrated that the  $L_s$ - $\alpha_I$  curve is nonlinear and showed that the extrapolation of data with relatively large separation regions may overestimate  $\alpha_I$  by as much as  $10^\circ$  at  $M=5.4$  as shown in Fig. 5.

#### Effect of Detection Method on Separation Results

More than one method has been used to detect separation by Roshko and Thomke [16], Law [17], Apples and Richards [25], Spaid and Frishett [26] and Rose et al. [24]. Roshko and Thomke [16] obtained consistent results for the incipient separation angle using orifice dams and the inflection in the curve for the variation in the pressure near the corner with  $\alpha$ . Law [17] investigated the effect of the experimental method used in the determination of the separation length on the incipient separation angle, as determined from the extrapolation of  $L_s$ - $\alpha$  curve to zero  $L_s$ . Figure 6 shows a comparison of the separation point location, as determined from four different procedures under different test conditions ( $M = 2.96$ ,  $\alpha = 14$ - $26^\circ$ ). In the first procedure, the separation point was identified with the first inflection point in the surface pressure distribution; in the second, it was determined from the shadowgraph; in the third, it was assumed at the oil accumulation line; and in the fourth method, the separation point was associated with the axial location, where there was an inflection point in

the  $p$  versus  $\alpha$  curve. Figure 5 shows that the separation length detected by all four methods are in agreement for large separated region. For small separation regions comparable with the boundary layer thickness, the oil flow predicts larger separated regions. It is clear from the figure that this difference translates into overpredicted incipient separation angles based on the surface pressure and shadowgraph data.

Delery and Marvin [1] distinguished between "true" incipient separation, corresponding to the first appearance of a separation bubble, and "effective" incipient separation, when the separation bubble starts to produce significant changes in the flow field. The first, which can be detected by surface flow visualization techniques, can be present without affecting the surface pressure according to Holden [10], Kuehn [12] and Settles et al. [18]. Figure 7 shows the difference between the "true" and "effective" incipient separation according to Rose et al. [24]. Holden [6] also distinguished between techniques for detecting the first appearance of reverse flow and other "pragmatic" methods, since each detects a different phenomena. The former techniques such as oil flow measurements, and measurements of surface shear and heat transfer, were used to detect the presence of separation in the sublayer. On the other hand, observing the inflection in the pressure distribution and the first appearance of a separation shock are pragmatic indicators of boundary layer separation. Hankey and Holden [3] suggested that turbulent boundary layer separation is a two stage process. The first separation is in the laminar sublayer with a laminar recirculation region at the base of the turbulent boundary layer. Next, a turbulent recirculation region is formed that increases rapidly with the interaction strength. This explains the abrupt change in the upstream influence which was observed by Holden [10] and by Elfstrom [7] when a

turbulent boundary layer separated over a highly cooled surface in hypersonic flow. More gradual separation was reported by Roshko and Thomke [16], Settles et al. [18] and Spaid and Frishett [26] for turbulent boundary layers in supersonic flows over adiabatic surfaces. In the latter case, the laminar sublayer had a greater influence on the development of separation with the increased interaction strength, as opposed to the weaker influence of the relatively thin laminar sublayer in the former case.

#### FLOW CHARACTERISTICS IN THE SEPARATED TURBULENT INTERACTION REGIONS

Holden [6] presented schlieren pictures of the two dimensional interactions for both externally generated incident shock and corner shock wave turbulent boundary layer interaction of various strengths. He gave a detailed description of the development of the separated regions with the increase in the interaction strength for both geometries. In both cases, Holden [6] determined that the viscous-inviscid interactions occurred almost entirely within the original boundary layer. The structures were similar for both Mach 8 and 13, with the interaction region and associated shocks becoming more embedded within the original boundary layer for the higher Mach number. For externally generated incident shocks, the separation initiates in the laminar sublayer. As the strength of the shock increases, the separation point moves forward from its initial location where the incident shock strikes the laminar sublayer, but remains downstream of the shock location at the boundary layer edge. In the case of compression corner, the induced separation shock originates at the bottom and combines with the reattachment shock within the boundary layer to form a single shock. The separation region elongates into the laminar sublayer, and when

the separation point is well forward of the junction, the plateau region is developed.

Kussoy and Horstman [30] obtained measurements in the interaction region of the turbulent boundary layer on a cone-ogive cylinder with an incident shock from a concentric annular shock generator at  $M = 7.2$  and  $Re_\delta = 0.2 \times 10^6$ . From their measurements at  $7.5^\circ$  and  $15^\circ$  generator angles, they developed sketches for the separated and unseparated shock wave turbulent boundary layer interactions as shown in Fig. 8. Under separated flow conditions, the flow turns as the boundary layer thins rapidly and the compression shock is formed. The decreased boundary layer thickness in the hypersonic interaction is associated with the large increase in the flow density.

Holden [6], Kussoy and Hortsman [30], Mikulla and Horstman [31], Dolling and Murphy [32], and Hayashi et al. [33] indicated that the separated regions were highly unsteady. Horstman and Owen [34] discussed the problem of detecting the separation and attachment points due to the unsteady nature of the separated flows. Holdman [6], whose results were obtained using high frequency response instruments, determined that the separation point oscillated in the streamwise direction at  $1-10 \text{ KHz}$  frequency and  $1/4 - 1/3 \delta$  amplitudes. Holden [3] and Dolling and Murphy [32] measured the fluctuations in the surface pressure in the interaction region for separated flows. Holden [10] measured surface pressure fluctuation levels up to the mean surface pressure.

Flow separation brings about changes in the surface pressure and heat transfer in the shock boundary layer interaction regions which must be taken into consideration in the design procedures. The bulk of the experimental



data available for code validation consists of the surface pressure and heat transfer measurements. Some mean flow measurements are also available, but the lack of turbulence measurements are attributed to the large errors in reducing the data in the separated regions of the shock boundary layer interactions.

Hayashi et al. [33] used an especially designed multilayered thin film gauge to measure the heat transfer fluctuations in the interaction region of an incident shock with a turbulent boundary layer for both separated and attached flows at  $M=4$ . The standard deviation in the heat transfer fluctuations were found to reach high local values that were double and almost ten times the upstream values in the unseparated and separated cases respectively. The variation in the standard deviation in the interaction region is shown in Figs. 9 and 10 for the two cases. The amplitude of the heat flux fluctuations peaks at the shock impinging point in the unseparated case, then decays rapidly downstream to the value before the interaction. In the separated case, a larger peak in the standard deviation is followed by two smaller peaks, then decays downstream to values higher than those upstream of the interaction. The sharp peak near the separation point was similar to the measured pressure fluctuations by Dolling and Murphy [32]. Intermittency of the fluctuations of heat transfer was observed near the separation point which was attributed to the separation shock wave oscillations.

#### Surface Measurements

Results of the experimentally measured surface pressure and heat transfer for separated hypersonic flow in a compression corner were reported by Holden [6, 10], Elfstrom [7], Coleman and Stollery [8] and by Kussoy and

Horstman [30]. Holden's results [6] for unseparated flow exhibit practically no upstream influence ahead of the compression corner on the surface pressure and heat transfer. The measurements obtained by Holden [10] in the interaction region of separated flows are given in Fig. 11. Both the pressure and heat transfer distributions are characterized by well defined plateaus in the recirculation region and large gradients in the separation and reattachment regions. The measured pressure plateau and the negative friction coefficient are both characteristics of the separated form.

When the flow was separated, the experimentally measured static pressures at the surface by Elfstrom [7] and Gray and Rhudy [11] reached very high local values before dropping rapidly to a value close to  $p_{inv}$ , the inviscid pressure the flow would attain if it were attached. The Mach numbers in these experiments ranged between 3.93 and 9.22. Elfstrom [7] attributed this hypersonic flow phenomena to the intersection of the separation and reattachment shock waves close to the surface. According to an inviscid flow model by Sullivan [35], the intersection of two shocks from a double wedge might result in a strong expansion wave, which explains the very high static pressures after the second shock.

Elfstrom's results [7] exhibited large overshoots in the pressure as the interaction strength increased as shown in Fig. 12. Coleman's results [8] showed correspondingly strong heat transfer overshoots (Fig. 13). Elfstrom [7] concluded that pressure overshoots are a hypersonic separated flow phenomena and suggested the disappearance of the overshoot as a criterion for incipient separation. The experimental results of Holden [6] and Roshko and Thomke [16] at higher Reynolds number exhibited only slight pressure overshoots. The results of the latter two investigators, at higher

Reynolds number, also differed from Elfstrom's results in the trend reversal in the incipient separation and separation length with the Reynolds number.

The surface pressure results of Holden [6,10] and Elfstrom [7] and the heat transfer measurements of Holden [6] and Coleman and Stollery [8] for corner flow show an increase in the upstream influence with the wedge angle. Elfstrom [7] studied in addition, the effect of the flow Mach number and the surface temperature on the measured surface pressure in a compression corner. As expected, his results indicate that increasing the free stream Mach number reduces the extent of the separated region. The measured peak surface pressure decreased with the wall temperature as shown in Fig. 14. The effect of wall temperature on the extent of the separation region was negligible in well separated flows, but a slight reduction of the interaction length was observed in separated flows at smaller deflection angles. When the flow was not separated, the effects of the Mach number and surface temperature on the surface pressure distribution were negligible [7]. Holden [6] reported a decrease in the separation length, while Elfstrom [7] reported the opposite effect with the Reynolds number. This is connected with the conflict regarding the trend reversal at high Reynolds number discussed earlier in convection incipient separation.

#### Flow Measurements

Kussoy and Horstman [30], presented the results of their detailed flow measurements in axisymmetric interactions of incident shock turbulent boundary layer interactions under separated and unseparated flow conditions. In both cases, an induced shock wave was caused by the lifting of the boundary layer, but its strength was significantly less for the attached case. Under these test conditions ( $M = 6.71$ ,  $T_w/T_\infty = 0.43$ ) the induced

shock eventually coalesced with the recompression shock further downstream as shown in Fig. 8. This is not in agreement with Holden's [3] description that the inviscid-viscous interactions and the induced and reattached shock coalescence occur within the original boundary layer. Based on their pitot and static pressure and total temperature surveys, Kussoy and Horstman [30] constructed the static pressure, velocity, and density contours. They also deduced the streamlines shown in Fig. 15a from the velocity and density profiles. The thinning of the boundary layer downstream of the separation bubble is evident in the figure. This is associated with the large increase in the flow density as shown in Fig. 15b, in which the incident, induced and recompression shock waves can be clearly recognized.

Mikulla and Horstman [31] presented the turbulence measurements in the separated and unseparated boundary layers for the same configuration. The measurements were obtained at four axial locations, the first upstream of the interaction influence, the second at the minimum wall skin friction for unseparated flow and the pressure plateau for separated flows, the third at the peak pressure and the fourth downstream of the interaction. The measurements are presented in Figs. 16a and 16b for the separated and unseparated flow cases. The data were not presented near the wall in the reversed flow region or in the region immediately above ( $0 < y/\delta < 0.25$ ), because the low Reynolds number in these zones were beyond the calibration range of the hot wires. The figures show that the rms mass flux  $\langle \rho u' \rangle / \rho \bar{u}$  exceeds 40% at shock impingement (location 2) and the rms vertical velocity  $\langle v' \rangle / \rho \bar{u}$  exceeds 30% at the same location in both separated and unseparated flows. The results demonstrate different lifetimes for the two flows, with the turbulence quantities returning to their pre-interaction values in the separated case, while the approach to equilibrium flow is more gradual in

the case of unseparated flow downstream of the interaction. The presented turbulence data were neither corrected for the interaction between the three turbulent velocity components, nor for the density and pressure fluctuations which could be important at these large turbulent intensities. The correction procedures used to account for these interactions required extensive measurements of third and fourth order correlations that were not obtained. The surface pressure measurements which were obtained by Holden [3] using high frequency response transducers indicated that the rms pressure fluctuations in the reattachment zone reached 20% of the free stream dynamic pressure.

Mikulla and Horstman [31] concluded that separation either destroys turbulence memory or inhibits the production of turbulence with a new equilibrium type boundary layer originating near reattachment. They proposed a coupling between the turbulent energy and the separation bubble unsteadiness, to account for the fact that the boundary layer relaxes to an equilibrium state much faster in the separated case than in the attached case. The detailed power spectra distributions of the measured fluctuating quantities supported their hypothesis.

#### Incipient Separation Correlations

Kessler et al. [15], Elfstrom [7] and Hankey and Holden [3] proposed different correlations for the condition of incipient separation. Elfstrom [7] demonstrated that Kessler's correlation severely overpredicted the separation trends at high Mach numbers ( $6.05 \leq M \leq 11.8$ ).

Elfstrom [7] proposed a simple model to predict the wedge angle at incipient separation. Referring to Fig. 17, his theory is based on the inviscid rotational analysis of the supersonic outer portion of the boundary

layer in the shock interaction region proposed by Roshko and Thomke [16]. Using the wake profile with the appropriate compressibility transformation, Elfstrom [7] determined the incipient separation angle based on the conjecture that the laminar sublayer separates when it encounters a normal shock. His model prediction and the experimental results of Kuehn [12], Gray and Rhudy [11] and Roshko and Thomke [16] are given in Fig. 18 which shows good agreement for Mach numbers in the range of 3 to 6. He also compared his model prediction for incipient separation angle with the cooled flow data at higher Mach numbers with good success (Fig. 19). One can see from Figs. 18 and 19 that his model predicts the trend reversal in incipient separation at high Reynolds numbers over a wide range of Mach numbers and wall temperatures.

Holden [10] suggested a correlation for the pressure ratio inducing separation in the form

$$\frac{P_I - P_o}{P_o} \propto C_{f_o} M_o^3 .$$

The experimental results from different sources are shown with the above correlation in Fig. 20. Holden based his correlation on viewing the separation mechanism in terms of the balance between the inertial and viscous forces at the wall. He arrived at this conclusion from the consistent pressure ratios in the shock and wedge induced separation in his experiments. The agreement between the experimental results of the two geometries in a large number of experimental studies is evident in Fig. 20.

### Separated Flow Correlations

Holden [6,10] found that the maximum measured pressures and heat transfer in separated hypersonic interaction are correlated by the following relation:

$$\frac{q_{\max}}{q_o} = \left( \frac{p_{\max}}{p_o} \right)^{.85}$$

The correlation is shown in Fig. 21 with the experimental data from different sources. Holden [3] also suggested the following correlation between the measured plateau pressure and heat transfer

$$\frac{q_{\text{plateau}}}{q_\gamma} = \left( \frac{p_{\text{plateau}}}{p_o} \right)^{5/8} .$$

The correlation is shown in Fig. 22 for shock and wedge induced separation for hypersonic flow.

## REFERENCES

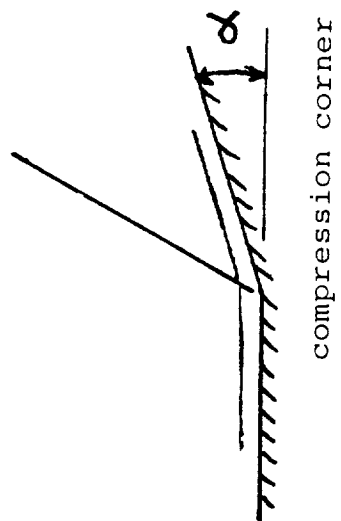
1. Delery, J. and Marvin, J.G., "Shock-Wave Boundary Layer Interactions," AGARD-AG-280, February 1986.
2. Delery, J., "Shock Boundary Layer Interaction and Its Control," Progress in Aerospace Sciences, Vol. 22, 1985, pp. 209-280.
3. Hankey, W.L. and Holden, M.S., "Two-Dimensional Shock-Wave Boundary Layer Interactions in High Speed Flows," AGARD-AG-203, June 1975.
4. Green, J.E., "Interactions Between Shock Waves and Turbulent Boundary Layers," Progress in Aerospace Sciences, Vol. 11, 1970, pp. 235-340.
5. Owen, F.K., "Measurements of Hypersonic Flow Fields," AGARD-FDP-VKI Special Course, Aerothermodynamics of Hypersonic Vehicles, May-June 1988.
6. Holden, M.S., "Shock Wave-Turbulent Boundary Layer Interactions in Hypersonic Flow," AIAA Paper No. 77-45, 1975.
7. Elfstrom, G.M., "Turbulent Hypersonic Flow at a Wedge-Compression Corner," Journal of Fluid Mechanics, Vol. 53, Part 1, 1972, pp. 113-127.
8. Coleman, G.T. and Stollary, J.L., "Heat Transfer from Hypersonic Turbulent Flow at a Wedge Compression Corner," Journal of Fluid Mechanics, Vol. 56, Part 4, 1972, pp. 741-752.
9. Batham, J.P., "An Experimental Study of Turbulent Separating and Reattaching Flows at a High Mach Number," Journal of Fluid Mechanics, Vol. 52, Part 3, April 1972, pp. 425-437.
10. Holden, M.S., "Shock Wave-Turbulent Boundary Layer Interaction in Hypersonic Flow," AIAA Paper No. 72-74, 1972.



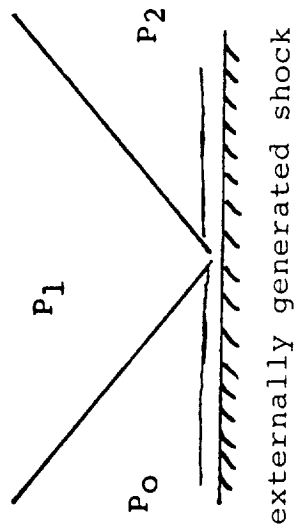
11. Gray, K.D. and Rhudy, R.W., "Investigation of Flat Plate Aspect Ratio Effects on Ramp Induced Adiabatic Boundary Layer Separation at Supersonic and Hypersonic Speeds," Final Report AEDC-TR-70-235, 1971.
12. Kuehn, D.M., "Experimental Investigation of the Pressure Rise Required for the Incipient Separation of Turbulent Boundary Layers in Two-Dimensional Supersonic Flow," NASA MEMO 1-21-59A, February 1959.
13. Drougge, G., "An Experimental Investigation of the Influence of Strong Adverse Pressure Gradients on Turbulent Boundary Layers at Supersonic Speeds," FFA Report 47, 1953.
14. Sterrett, J.P. and Emery, J.C., "Experimental Separation Studies for Two Dimensional Wedges and Curved Surfaces at Mach Numbers of 4.8 to 6.2," NASA TN D-1014 (1962).
15. Kessler, W.C., "Supersonic Turbulent Boundary Layer Interaction with an Expansion Fan and a Compression Corner, MDC E0264, December 1970.
16. Roshko, A. and Thomke, G.J., "Supersonic Turbulent Boundary Layer Interaction with a Compression Corner at Very High Reynolds Number," Proceedings of the 1969 Symposium on "Viscous Interactions Phenomena in Supersonic and Hypersonic Flows", University of Dayton Press, 1964, pp. 109-133.
17. Law, H.C., "Supersonic Turbulent Boundary Layer Separation Measurements at Reynolds Numbers of  $10^7$  to  $10^8$ ," AIAA Journal, Vol. 12, No. 6, 1974, pp. 794-797.
18. Settles, G.S., Bogdonoff, S.M. and Vas, I.E., "Incipient Separation of a Supersonic Turbulent Boundary-Layer at Moderate to High Reynolds Numbers," AIAA Journal, Vol. 14, No. 1, 1976, pp. 50-56.

19. Bushnell, D.M., Johnson, C.B., Harvey, W.D. and Feller, W.V.,  
"Comparison of Prediction Methods and Studies of Relaxation in  
Hypersonic Turbulent Boundary Layers," Turbulent Boundary Layer  
Conference Proceedings, NASA Langley Research Center, December 1968.
20. Gulbran, C.E., Redeker, E., Miller, D.S. and Strack, S.L., "Heating in  
Regions of Interfering Flow Fields, Part III: Two Dimensional  
Interaction Caused by Plane Shocks Impinging on Flat Plate Boundary  
Layers," AFFDL-TR-65-49, March 1967.
21. Fernholz, H.H. and Finley, P.J., "A Critical Compilation of  
Compressible Turbulent Boundary Layer Data," AGARDograph No. 223, June  
1977.
22. Coleman, G.T. and Stollery, J.L., "Incipient Separation of Axially  
Symmetric Hypersonic Turbulent Boundary Layers," AIAA Journal, Vol. 12,  
1974, pp. 119-120.
23. Kuehn, D.M., "Turbulent Boundary Layer Separation Induced by Flares on  
Cylinders at Zero Angle of Attack," NASA TR 117, 1961.
24. Rose, W.C., Page, R.J. and Childs, M.E., "Incipient Separation Pressure  
Rise for a Mach 3.8 Turbulent Boundary Layer," AIAA Journal, Vol. 11,  
No. 5, 1973, pp. 761-763.
25. Apples, C. and Richards, B.E., "Incipient Separation of a Compressible  
Turbulent Boundary Layer," AGARD CP-168, Flow Separation, may 1975.
26. Spaid, F.W. and Frishett, J.C., "Incipient Separation of a Supersonic,  
Turbulent Boundary Layer, Including Effects of Heat Transfer," AIAA  
Journal, Vol. 10, No. 7, July 1977, pp. 915-922.
27. Green, J.W., "Reflection of an Oblique Shock Wave by a Turbulent  
Boundary Layer," Journal of Fluid Mechanics, Vol. 40, Part 1, 1970, pp.  
81-95.

28. Holloway, P.F., Sterrett, J.R. and Greekmore, H.S., "An Investigation of Heat Transfer Within Regions of Separated Flow at a Mach Number of 6.0," NASA TND-3074, 1965.
29. Gadd, G.E., Cope, W.F. and Attridge, J.L., "Heat-Transfer and Skin-Friction Measurements at a Mach Number of 2.44 for a Turbulent Boundary Layer on a Flat Surface and in Regions of Separated Flow," R&M No. 3148, British Aeronautical Research Council, 1960.
30. Kussoy, M.I. and Horstman, C.C., "An Experimental Documentation of a Hypersonic Shock-Wave Turbulent Boundary-Layer Interaction Flow - With and Without Separation," NASA TM X-62, 412, 1975.
31. Mikulla, V. and Horstman, C.C., "Turbulence Measurements in Hypersonic Shock-Wave Boundary-Layer Interaction Flows," AIAA Journal, Vol. 14, No. 5, 1976, pp. 568-575.
32. Dolling, D.S. and Murphy, M.T., "Unsteadiness of the Separation Shock Wave Structure in a Supersonic Compression Ramp Flow Field," AIAA Journal, Vol. 21, No. 9, 1983, pp. 1628-1634.
33. Hayashi, M., Aso, S. and Tan, A., "Fluctuation of Heat Transfer in Shock Wave/Turbulent Boundary-Layer Interaction," AIAA Journal, Vol. 27, No. 4, 1989, pp. 399-404.
34. Horstman, C.C. and Owen, F.K., "New Diagnostic Technique for the Study of Turbulent Boundary-Layer Separation," AIAA Journal, Vol. 12, No. 10, 1974, pp. 1436-1438.
35. Sullivan, P.A., "Hypersonic Flow Over Slender Double Wedges," AIAA Journal, Vol. 7, 1963, pp. 1927.



compression corner



externally generated shock

FIG. 1. FLOW CONFIGURATIONS

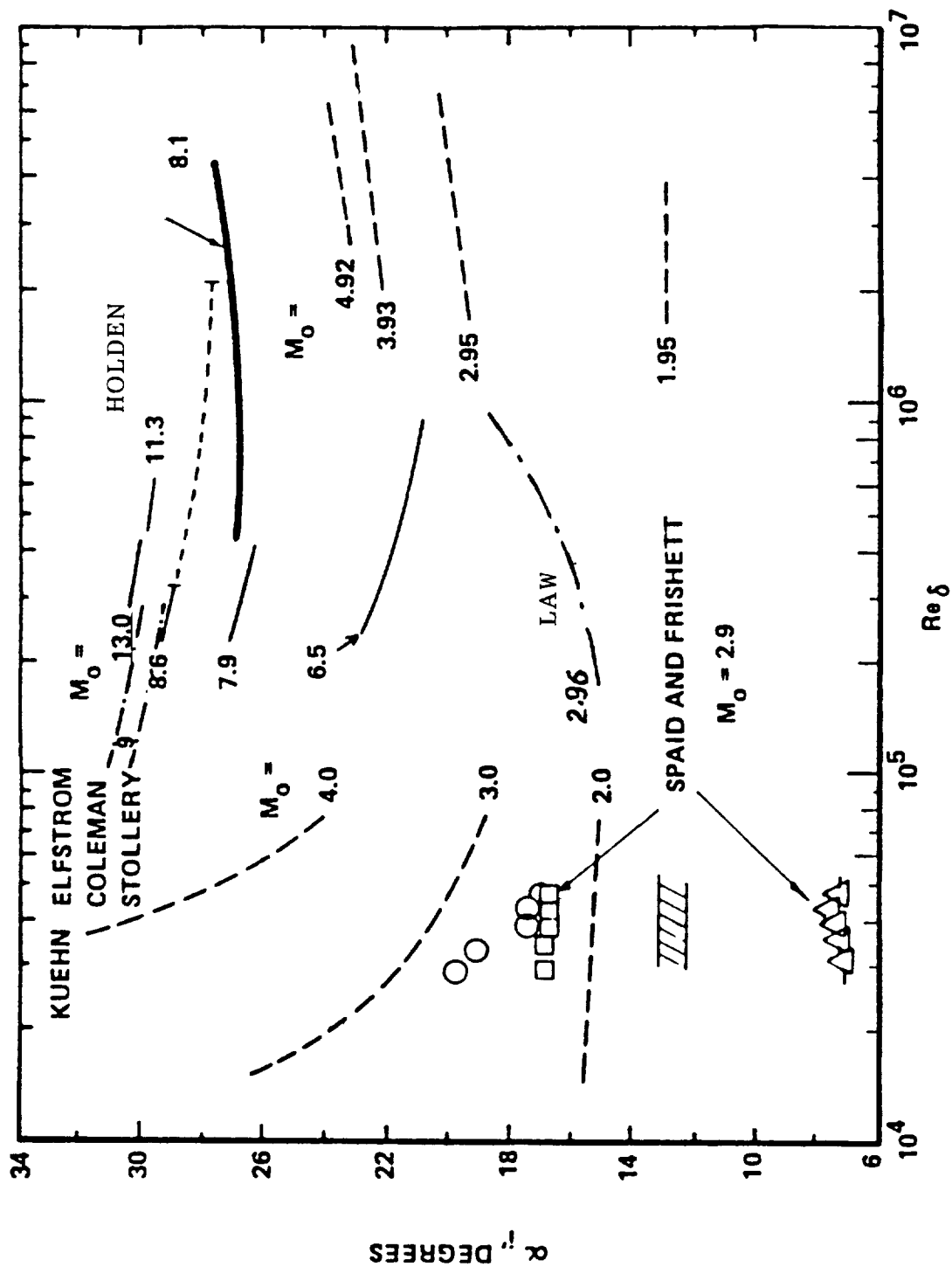


FIG. 2. WEDGE ANGLE TO INDUCE INCIPIENT SEPARATION

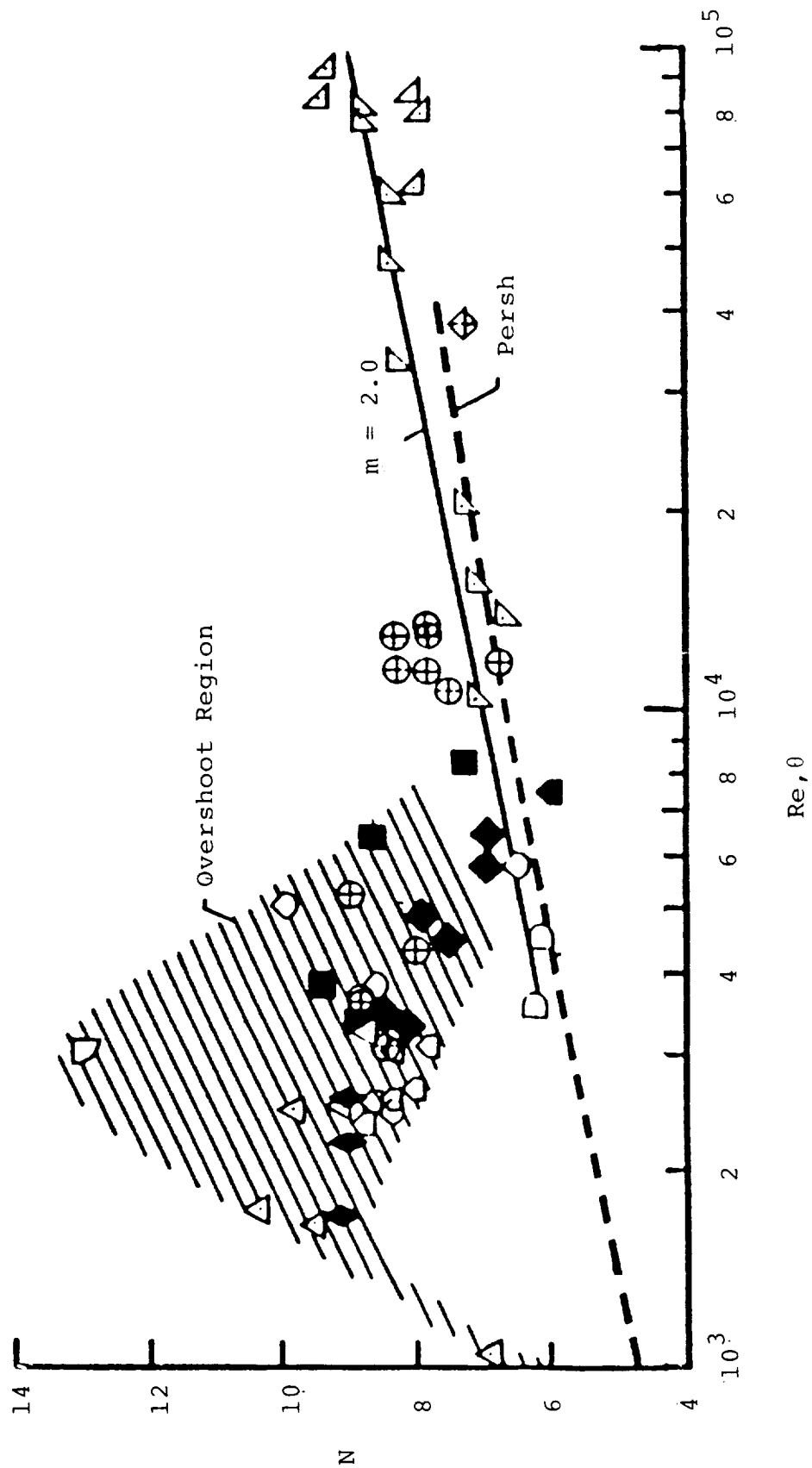


FIG. 3. VARIATION OF  $N$  WITH  $Re, \theta$  FOR FLAT PLATES, CONES AND HOLLOW CYLINDERS (REF. 19).

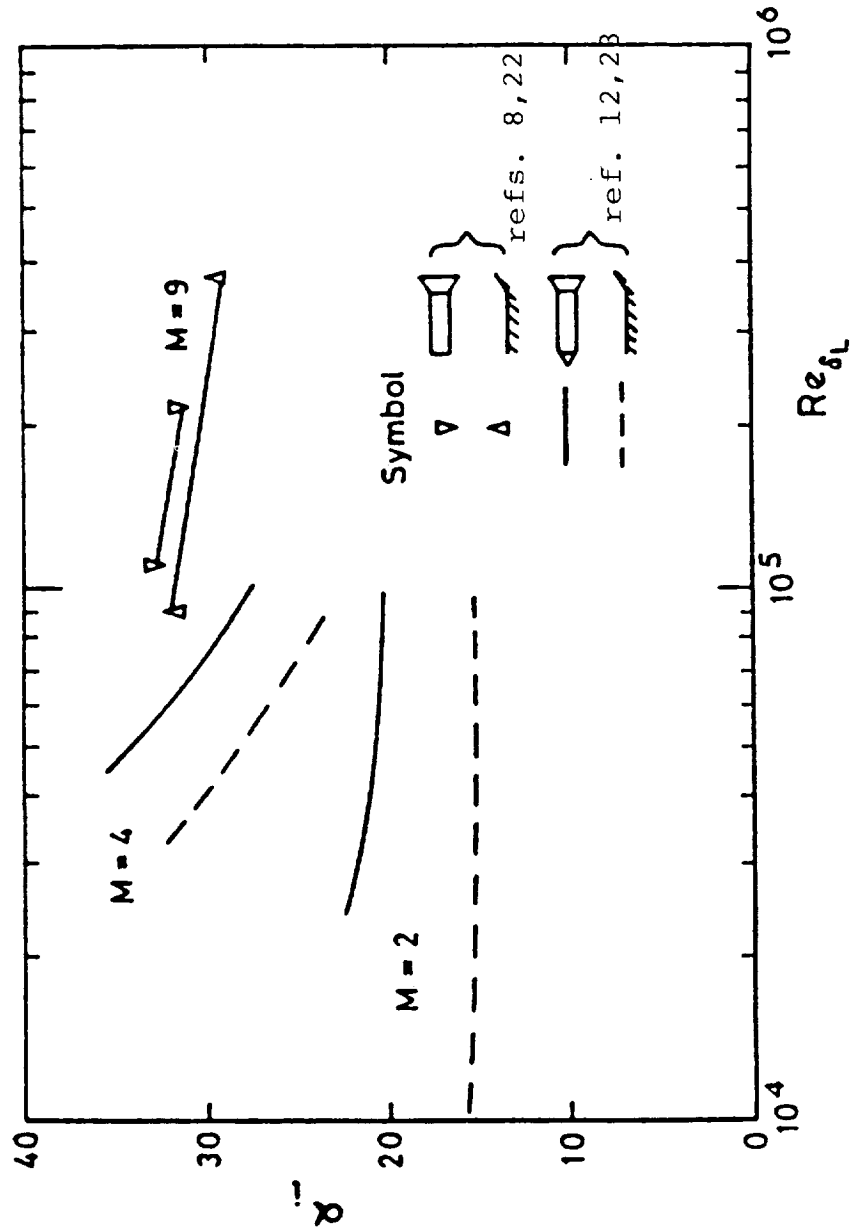
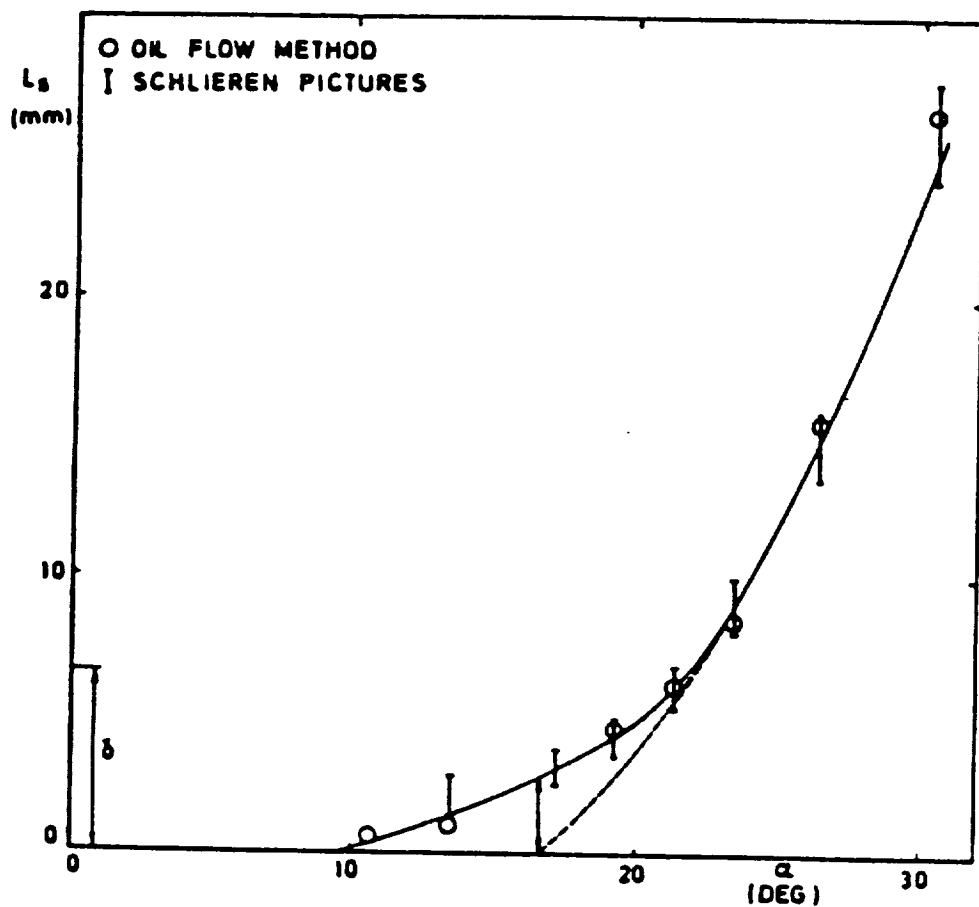
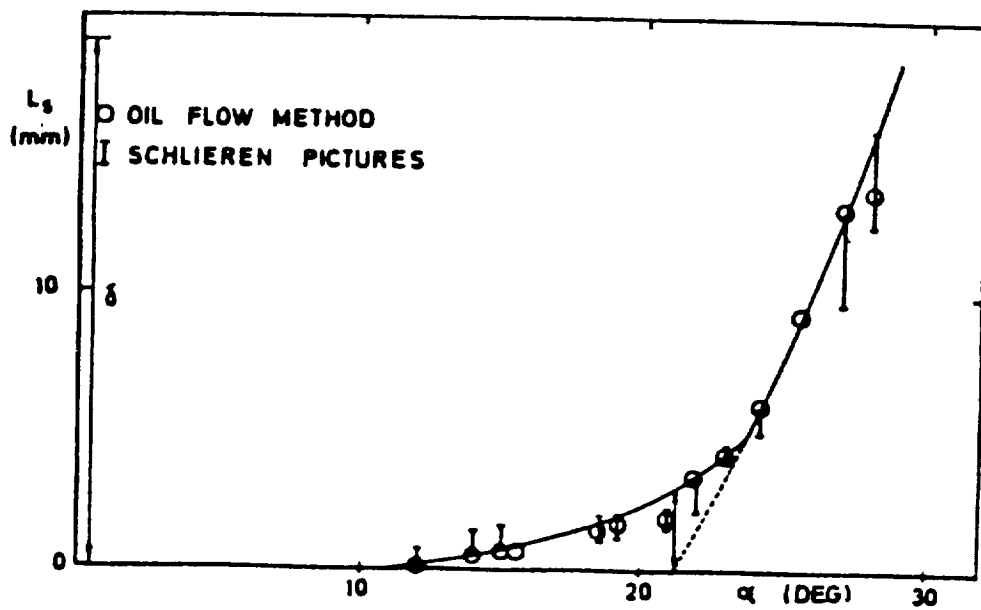


FIG. 4. COMPARISON WITH WEDGE COMPRESSION CORNER RESULTS  
 INCIPIENT SEPARATION ON A CYLINDER-FLARE (REF. 22).



(a)  $M = 3.5$ ,  $Re_\delta = 2.07 \times 10^5$



(b)  $M = 5.4$ ,  $Re_\delta = 6.67 \times 10^5$

FIG. 5. SEPARATION DISTANCE AS FUNCTION OF WEDGE ANGLE (REF. 25).



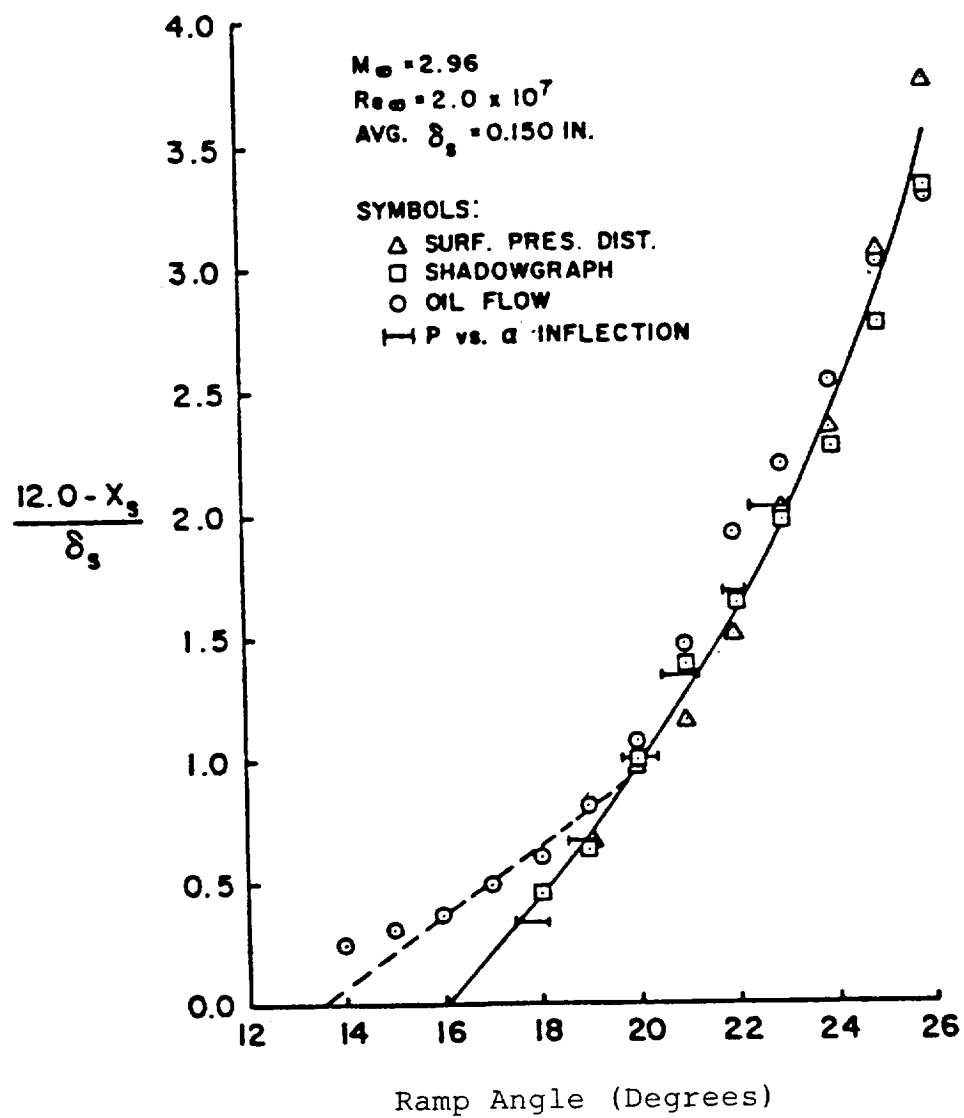


FIG. 6. VARIATION OF SEPARATION DISTANCE WITH COMPRESSION RAMP ANGLE. (REF. 17).

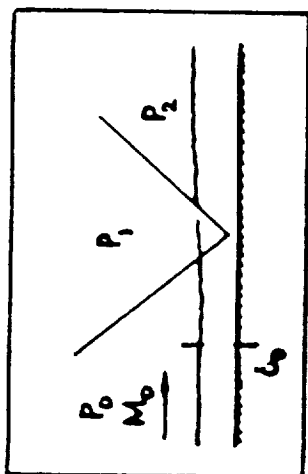
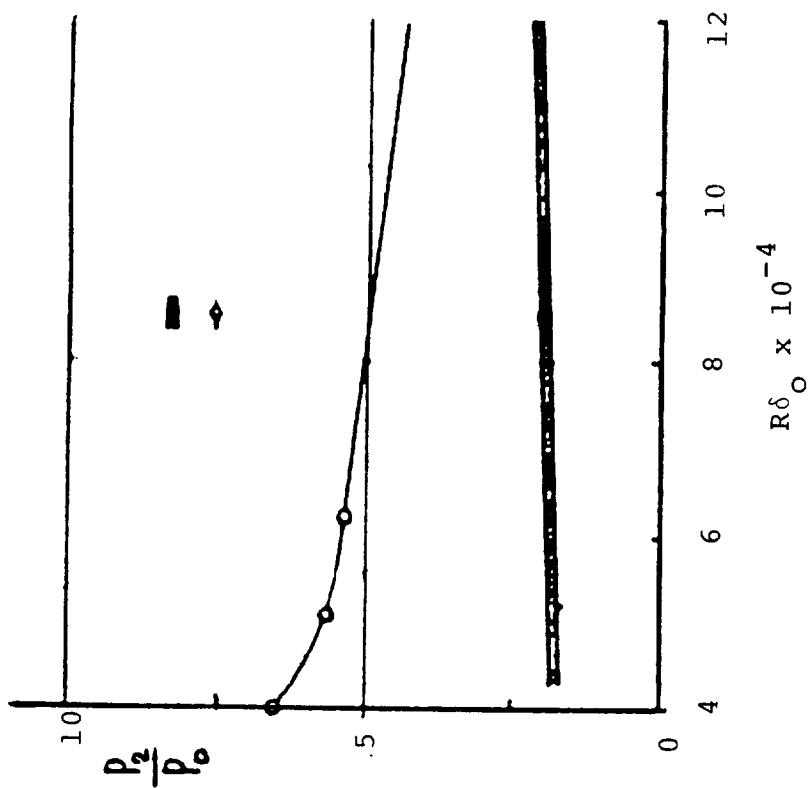


FIG. 7. DIFFERENCE BETWEEN "TRUE" AND "EFFECTIVE" INCIPIENT SEPARATION (REF. 24).

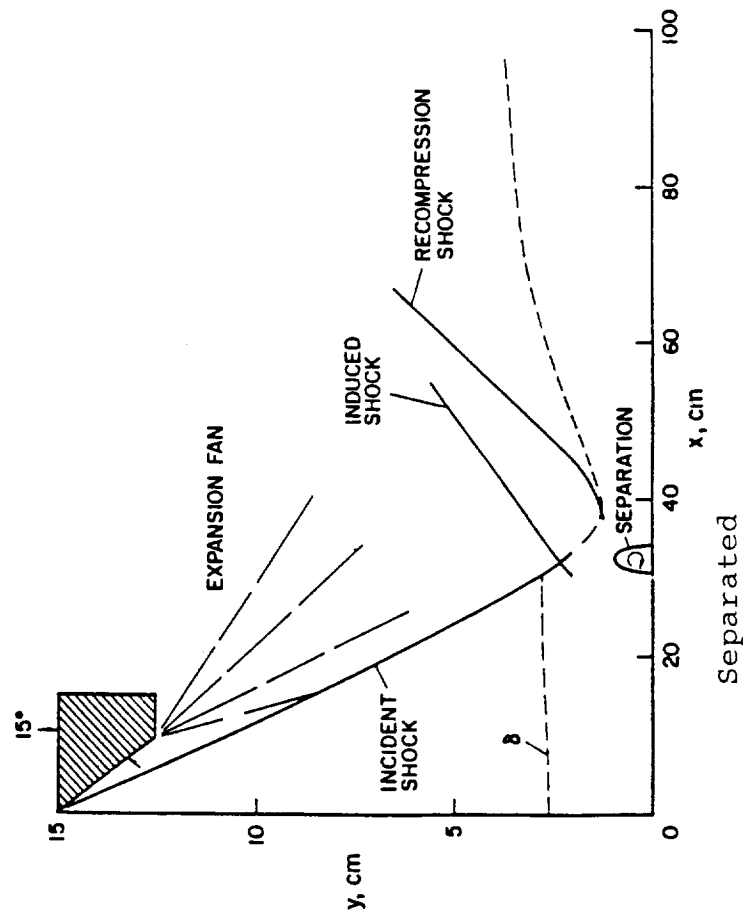
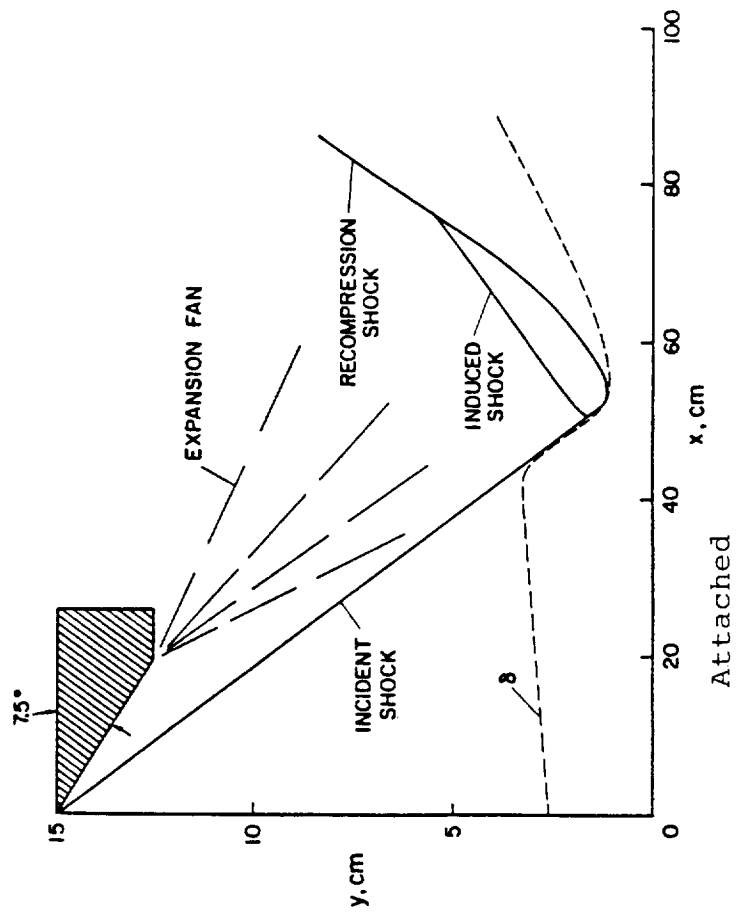


FIG. 8. FLOW FIELD SCHEMATIC (REF. 30).

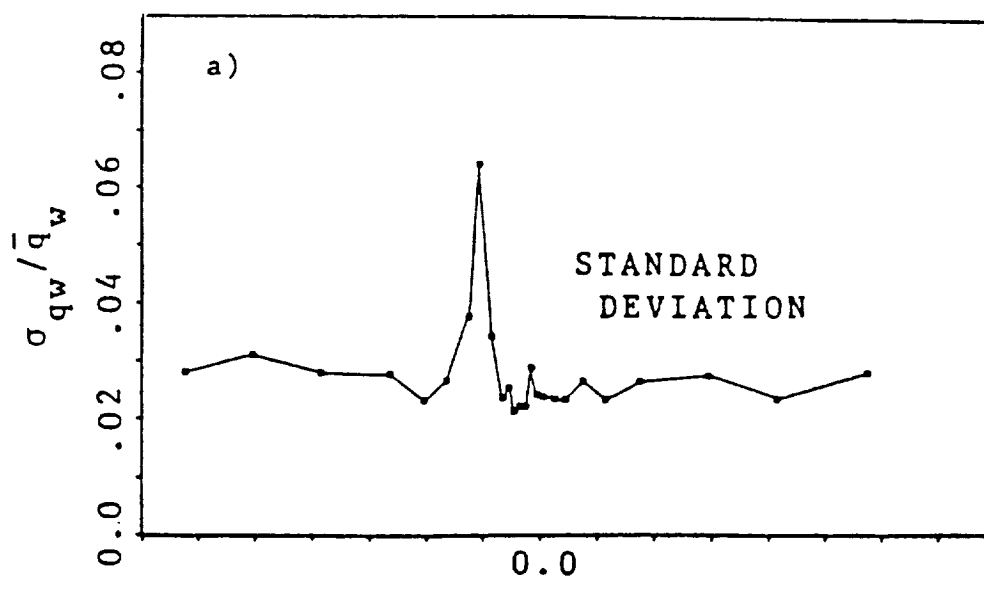


FIG. 9. HEAT FLUX STANDARD DEVIATION IN THE UNSEARATED INTERACTION,  $M_\infty = 18.5$ ,  $Re_L = 1.26 \times 10^7$ ,  $T_w/T_O = 0.56$ ,  $\beta = 18.5$ ,  $T_O = 540$  (REF. 33).

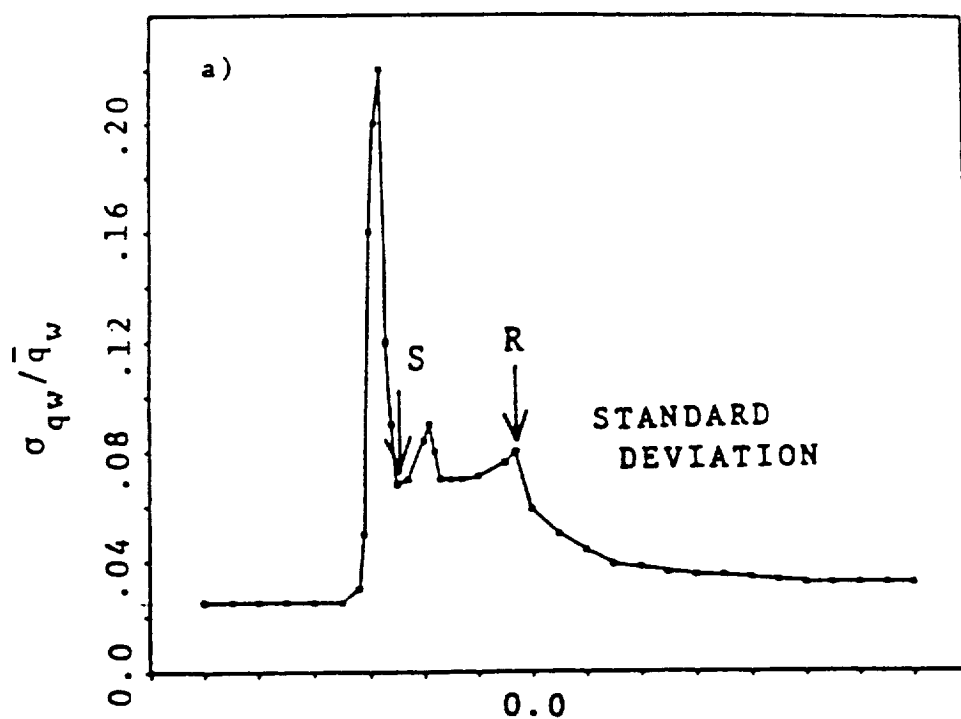


FIG. 10. HEAT FLUX STANDARD DEVIATION IN THE SEPARATED INTERACTION,  $M_\infty = 3.89$ ,  $Re_L = 1.26 \times 10^7$ ,  $T_w/t_O = 0.57$ ,  $\beta = 22.3$ ,  $T_O = 535$  (REF. 33).

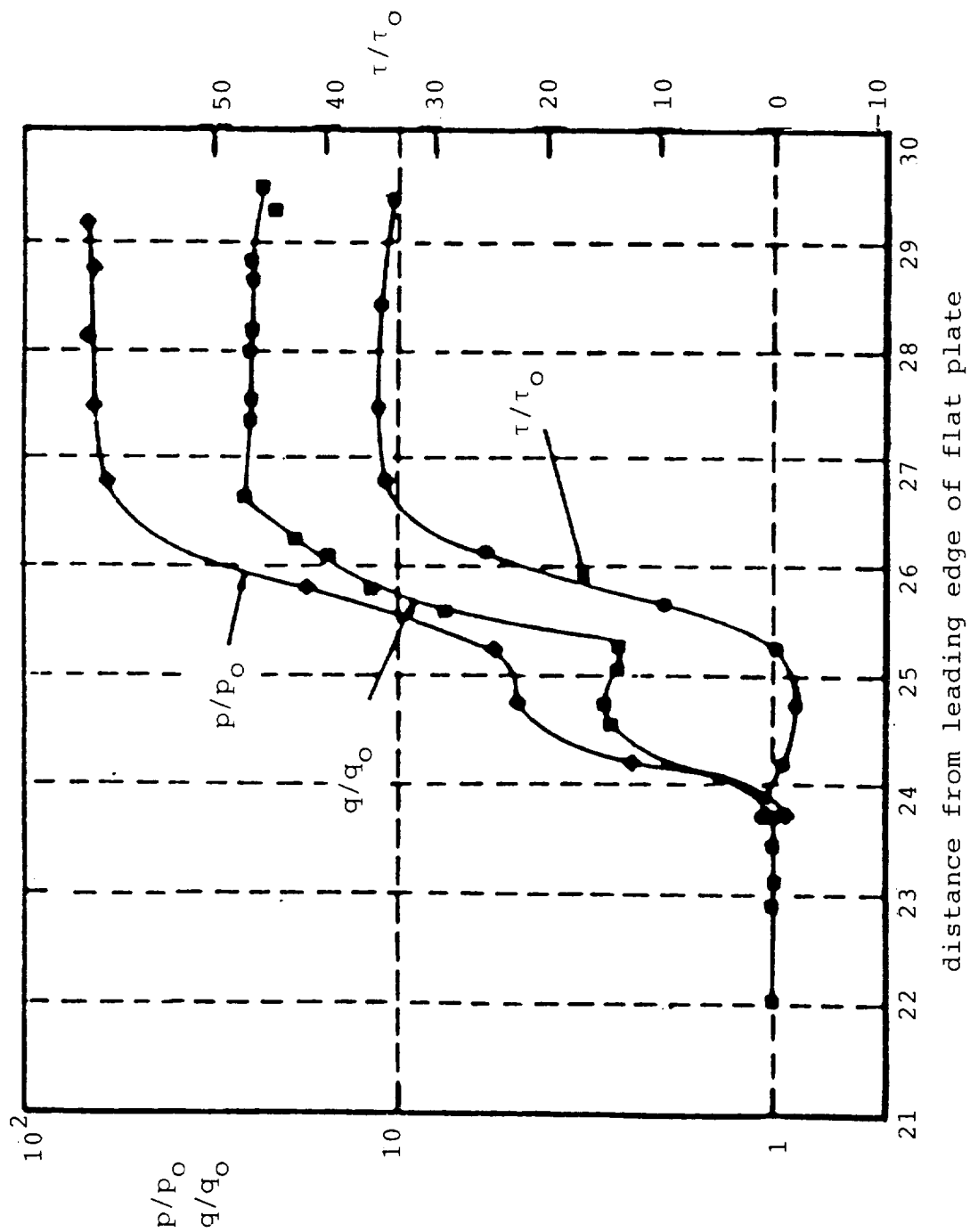


FIG. 11. PRESSURE, HEAT TRANSFER AND SKIN FRICTION DISTRIBUTION,  
 $M = 8.7$ ,  $Re_L = 30 \times 10^6$  (Ref. 3).

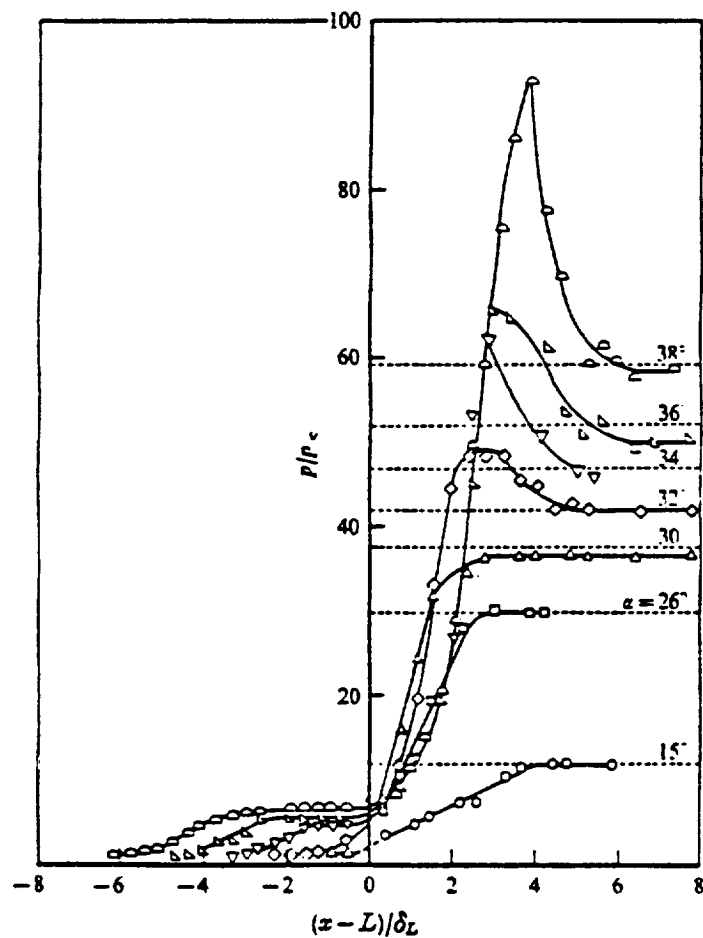
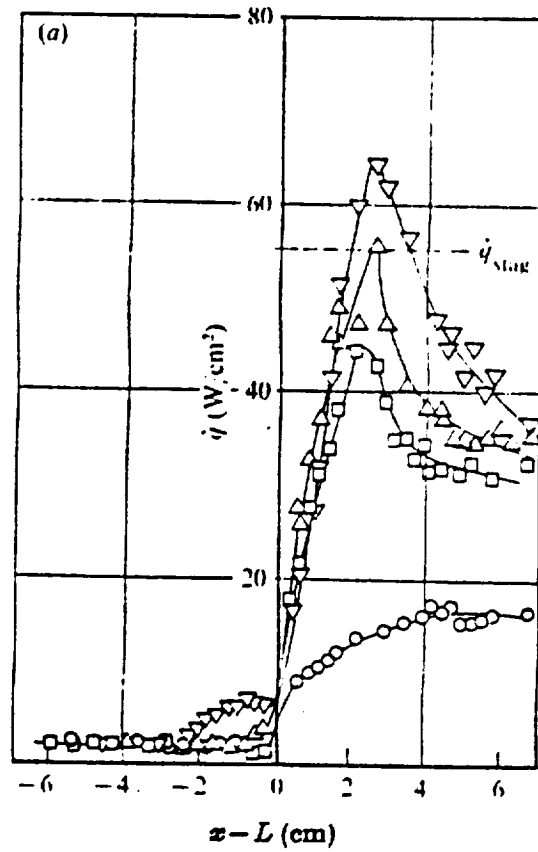


FIG. 12. STATIC PRESSURE DISTRIBUTION AT A WEDGE-COMPRESSION CORNER,  $M = 9.22$ ,  $Re_{\delta_L} = 4 \times 10^5$ ,  $T_o = 1070^\circ K$ ,  $T_w = 295^\circ K$  (REF. 7).

	$\circ$	$\nabla$	$\nabla$	$\diamond$	$\triangle$	$\square$	$\circ$
$\alpha$	$38^\circ$	$36^\circ$	$34^\circ$	$32^\circ$	$30^\circ$	$26^\circ$	$15^\circ$

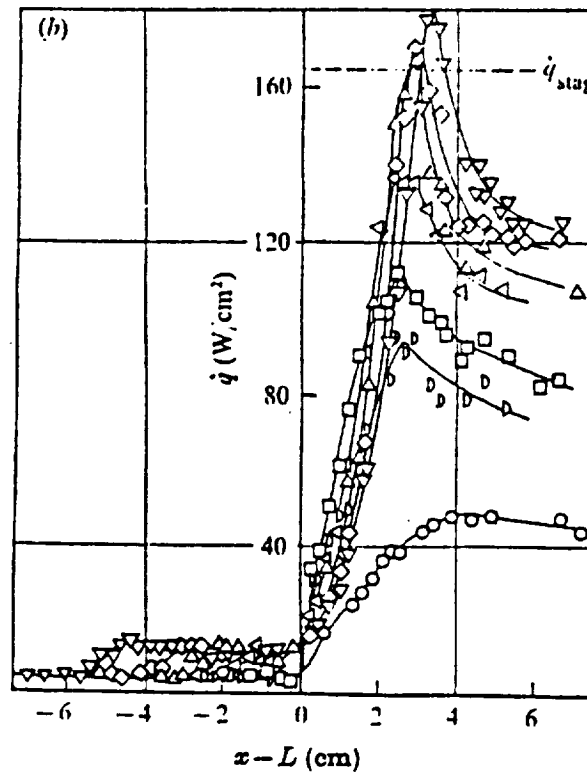


$$M_{\infty} = 8.96$$

$$Re_{\infty} = 1.2 \times 10^5 \text{ cm}^{-1}$$

$$T_O = 1070^\circ\text{K}$$

$$T_W = 295^\circ\text{K}$$



$$M_{\infty} = 9.22$$

$$Re_{\infty} = 4.7 \times 10^5 \text{ cm}^{-1}$$

$$T_O = 1070^\circ\text{K}$$

$$T_W = 295^\circ\text{K}$$

FIG. 13. HEAT TRANSFER RATE MEASUREMENT AT A WEDGE COMPRESSION CORNER (REF. 8).

$\alpha$      $\nabla$   $38^\circ$      $\diamond$   $36^\circ$      $\triangle$   $34^\circ$      $\triangleleft$   $32^\circ$      $\square$   $30^\circ$      $\circ$   $26^\circ$      $\bigcirc$   $15^\circ$

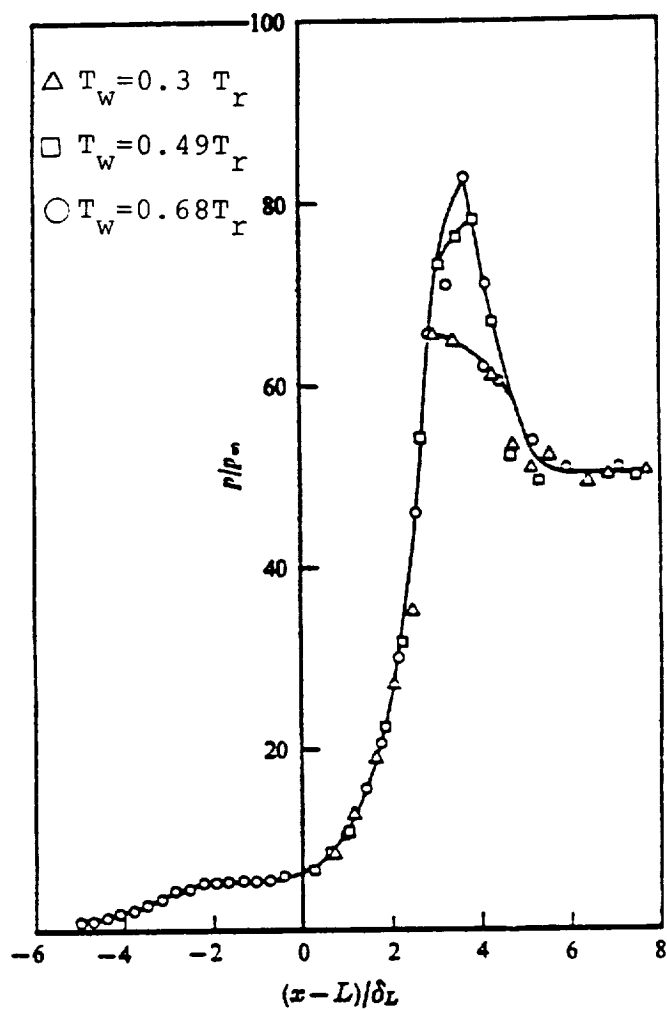


FIG. 14. EFFECT OF WALL TEMPERATURE ON A SEPARATED  
 FLOW STATIC PRESSURE DISTRIBUTION,  
 $M_\infty = 9.22$ ,  $Re_{\delta_L} \approx 4 \times 10^5$ ,  $\alpha = 36^\circ$  (REF. 7).



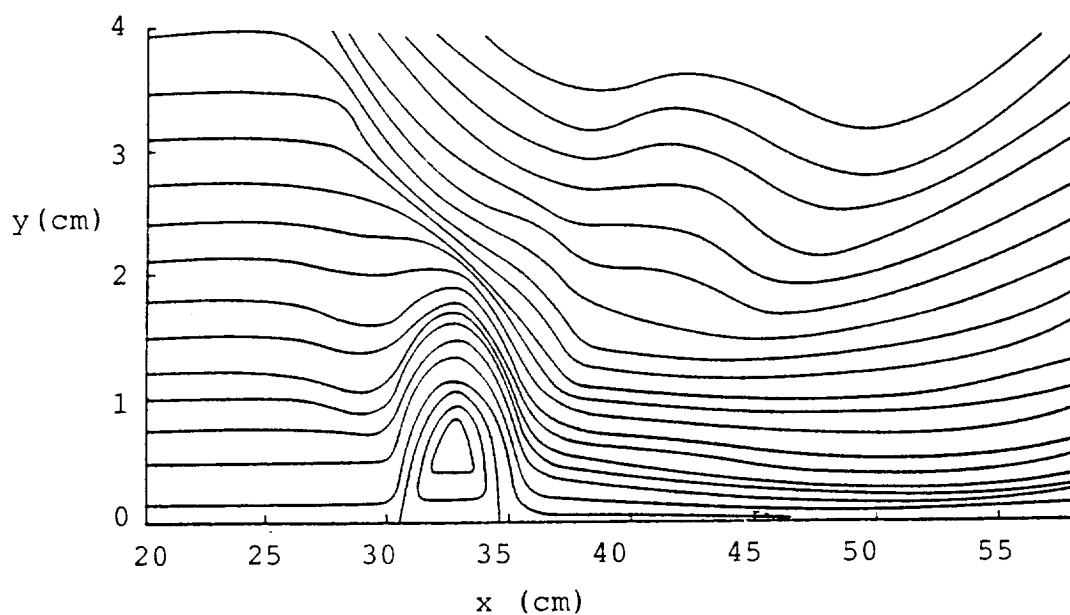


FIG. 15a. STREAMLINE CONTOURS,  $\alpha = 15^\circ$ ,  $M_\infty = 6.86$ ,  
 $T_w/T_{O_\infty} = 0.43$  (REF. 30)

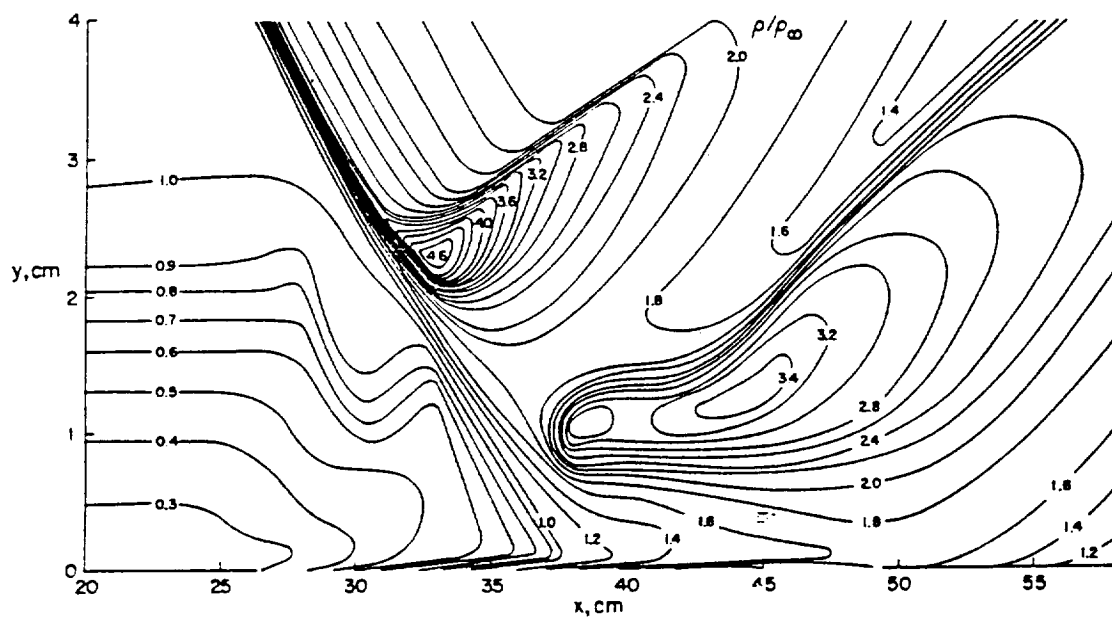


FIG. 15b. DENSITY CONTOURS,  $\alpha = 15^\circ$ ,  $M_\infty = 6.86$ ,  $T_w/T_{O_\infty} = 0.43$   
 (REF. 30).

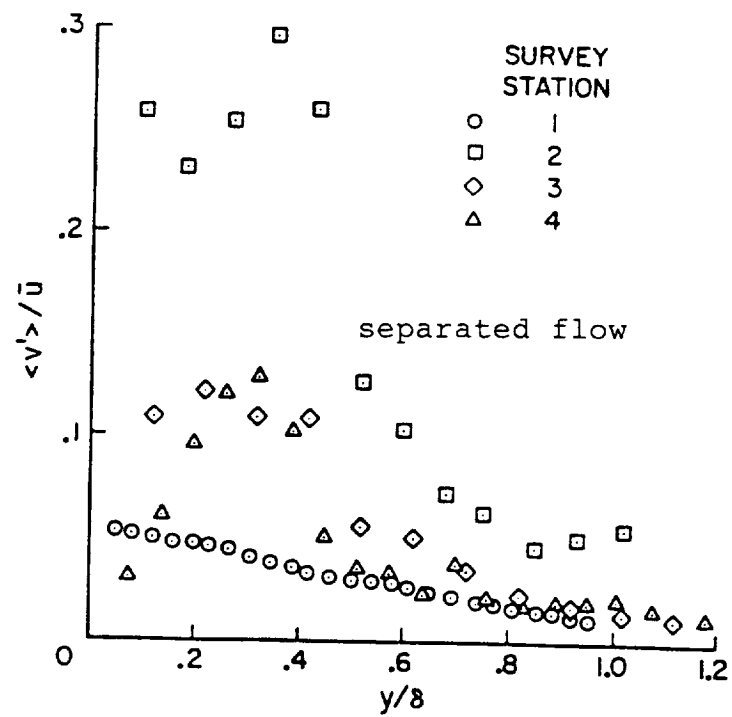
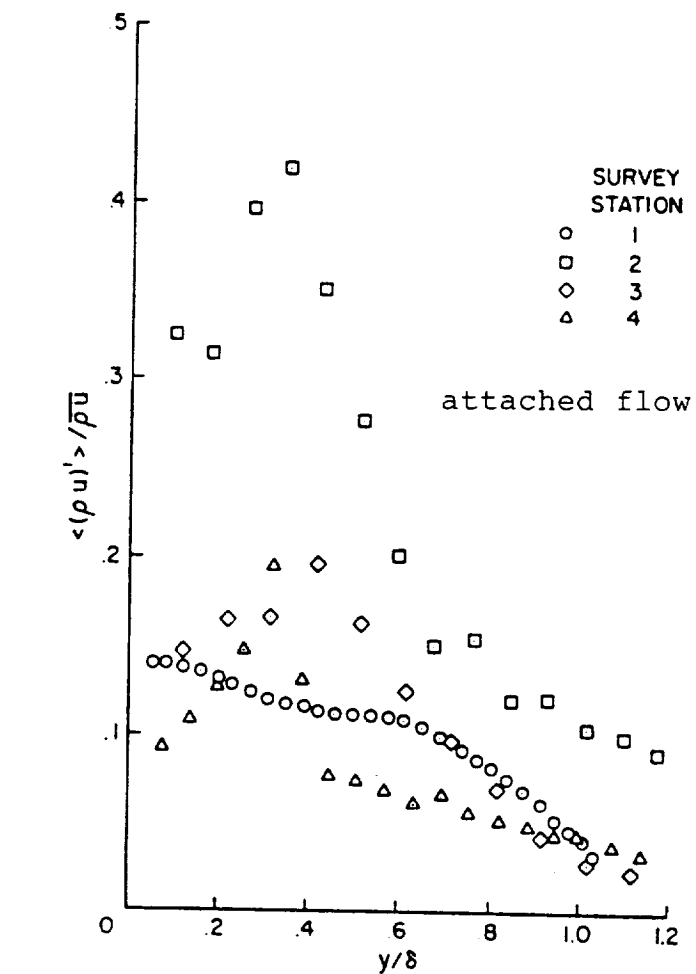


FIG. 16. RMS MASS-FLUX DISTRIBUTIONS (REF. 31).

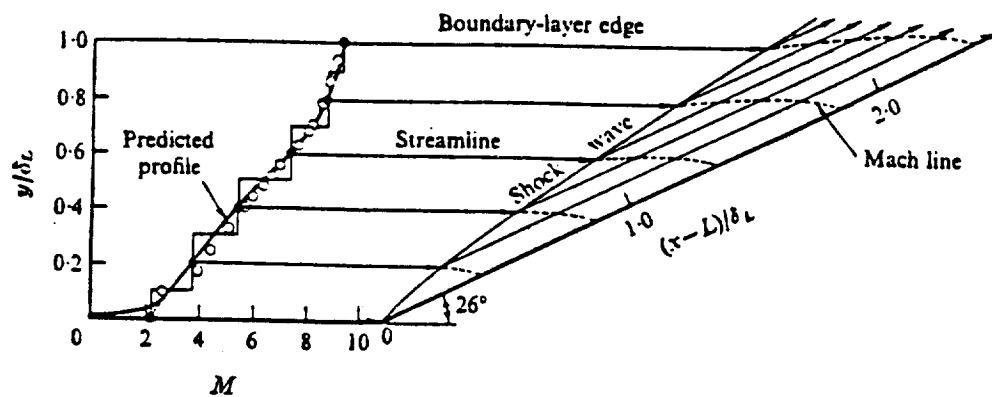


FIG. 17. INVISCID ROTATIONAL FLOW MODEL (REF. 7).

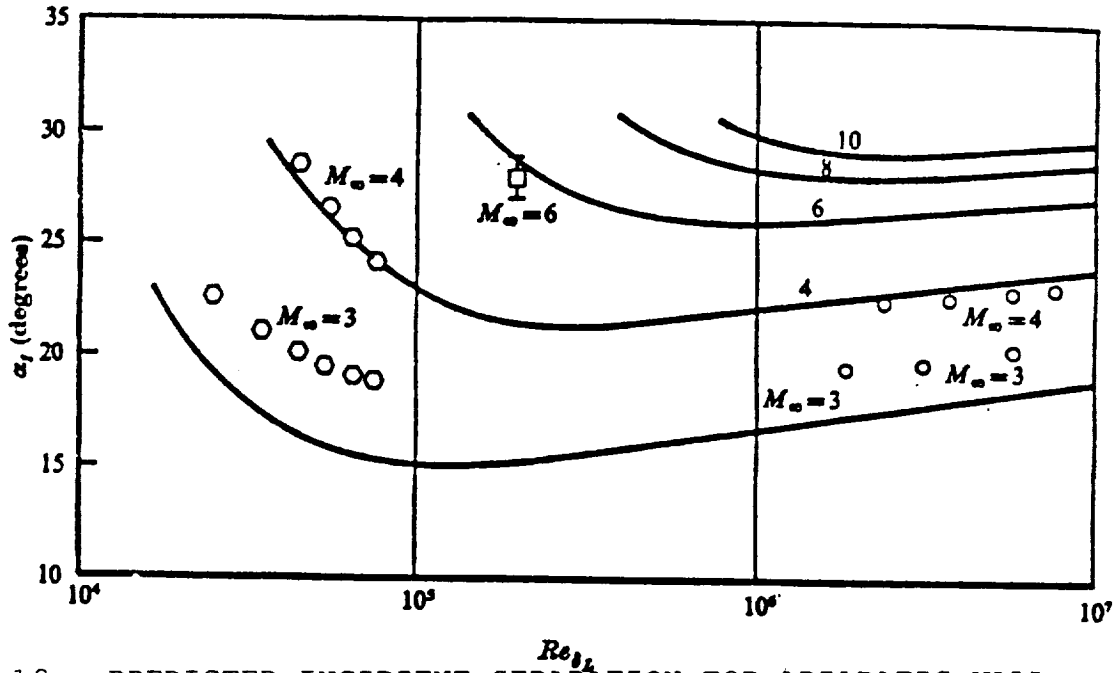


FIG. 18. PREDICTED INCIPIENT SEPARATION FOR ADIABATIC WALL CONDITIONS. EXPERIMENT:  $\circ$ , KUEHN (1959);  $\square$ , GRAY & RHUDY (1971);  $\circ$ , THOMKE & ROASKO (1969) (REF. 7)

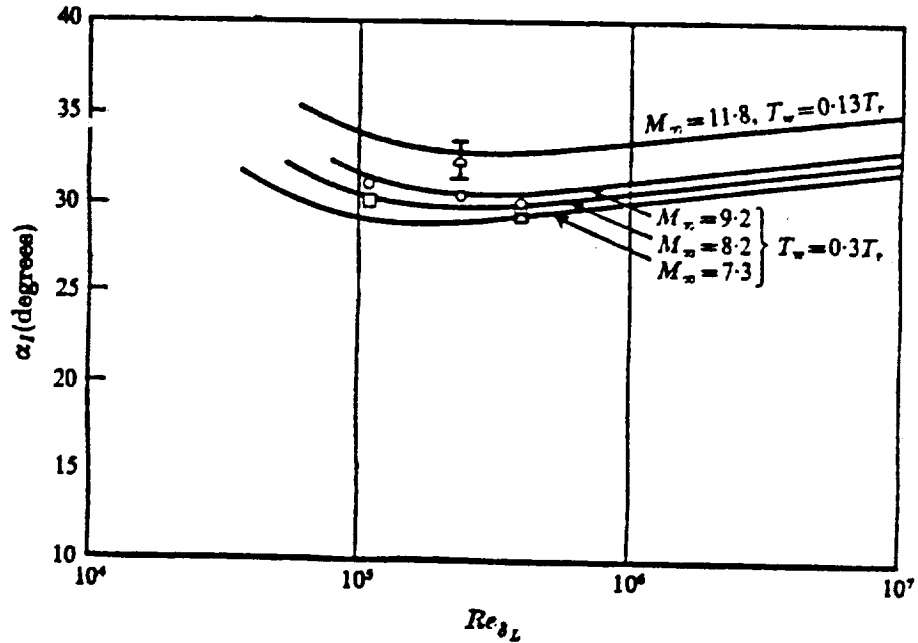


FIG. 19. PREDICTED INCIPIENT SEPARATION FOR NON-ADIABATIC WALL CONDITIONS. EXPERIMENT:  $\triangle$ , APPELS & BACKX (1971),  $M_\infty = 11.8$ ,  $T_w = 0.13 T_\infty$ ;  $\circ$ , ELFSTROM (1972),  $M_\infty = 9$ ,  $T_w = 0.3 T_\infty$ ;  $\square$ , ELFSTROM (1972),  $M_\infty = 8.2$ ,  $T_w = 0.3 T_\infty$ ;  $\triangle$ , ELFSTROM (1972),  $M_\infty = 7.3$ ,  $T_w = 0.3 T_\infty$  (REF. 7).

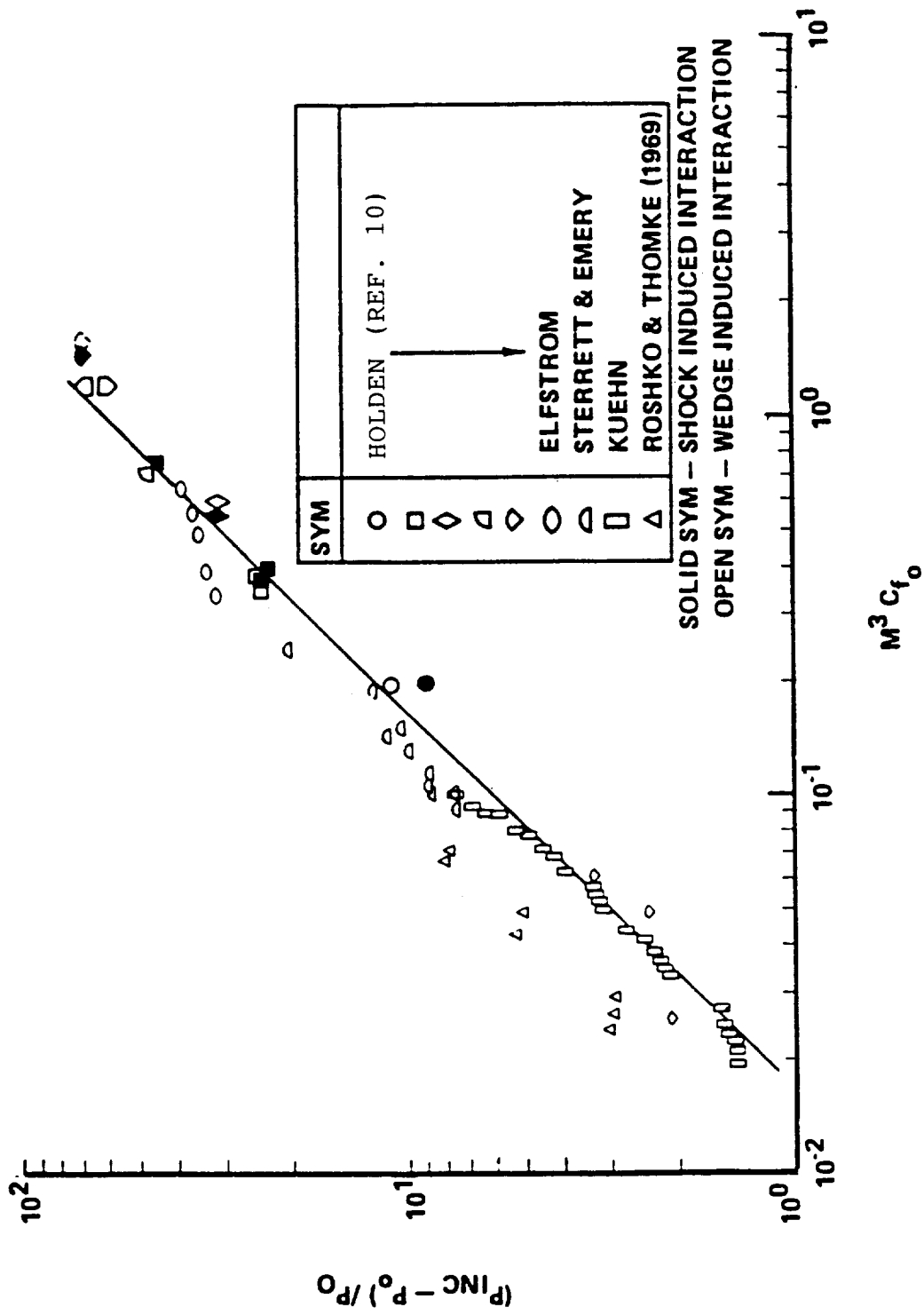


FIG. 20. CORRELATION OF MAXIMUM HEATING IN WEDGE AND EXTERNALLY GENERATED SHOCK-INDUCED TURBULENT SEPARATED FLOWS, (REF. 10).

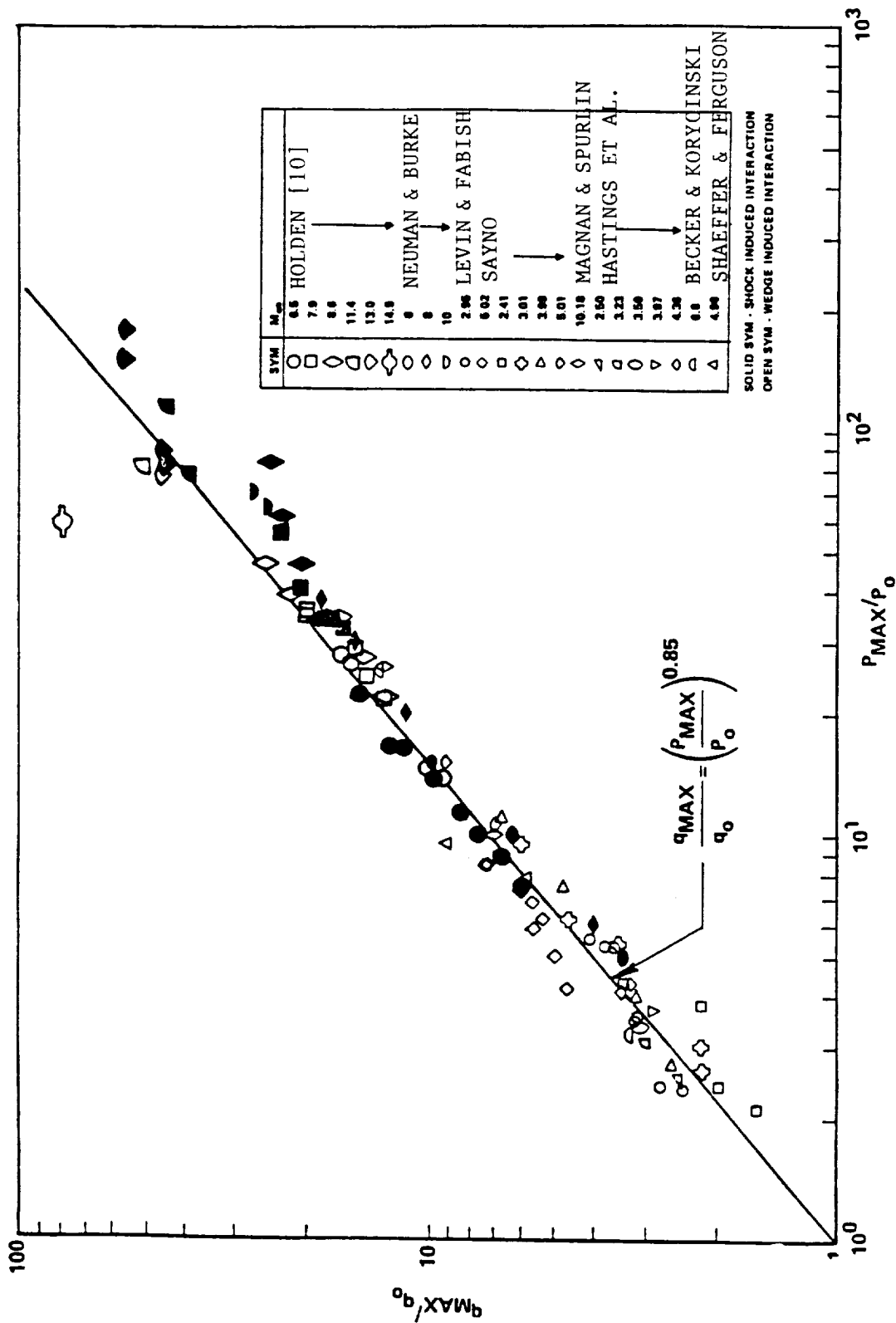


FIG. 21. CORRELATION OF MAXIMUM HEATING IN WEDGE - AND EXTERNALLY GENERATED SHOCK-INDUCED TURBULENT SEPARATED FLOWS (REF. 10).

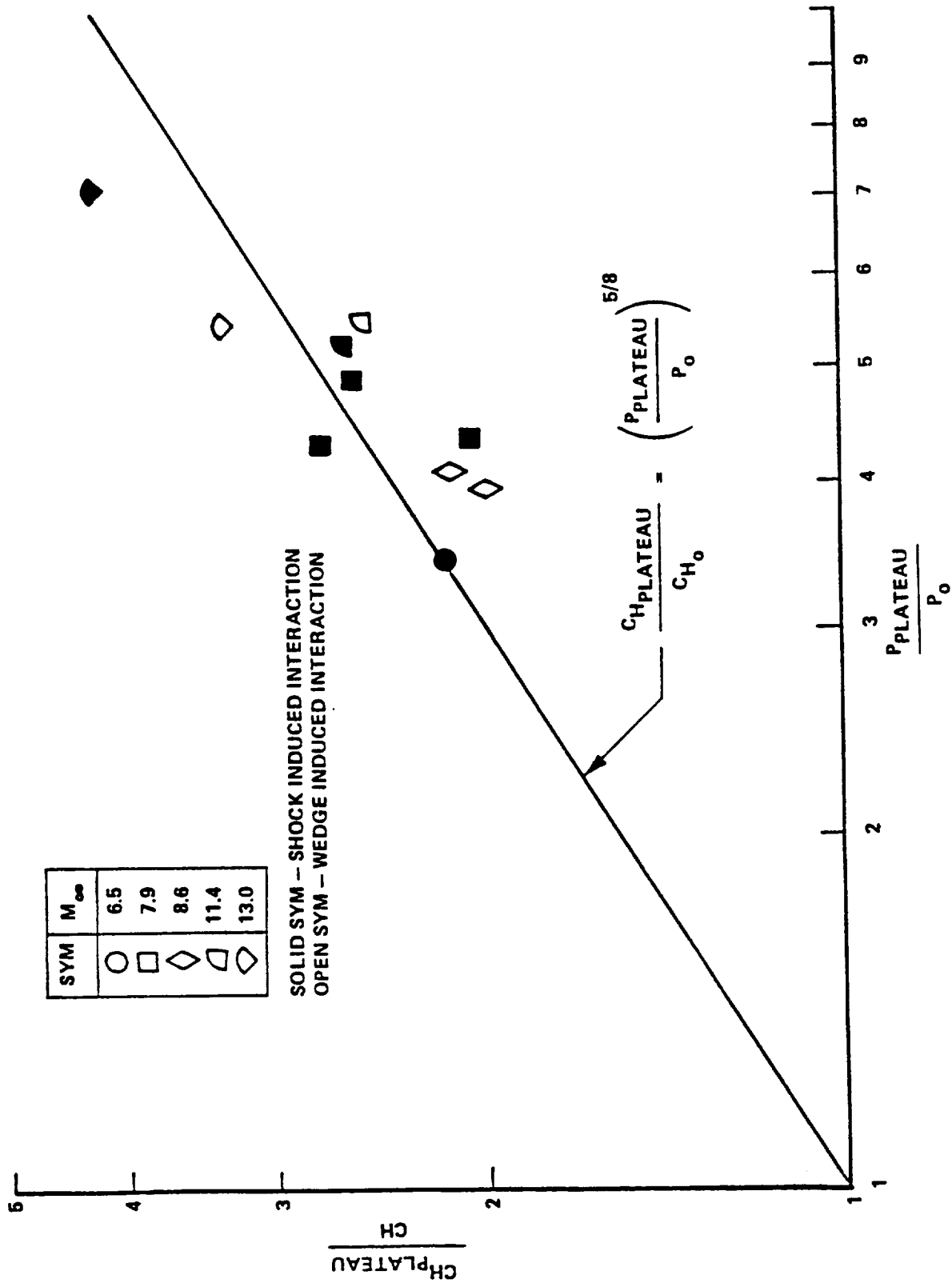


FIG. 22. CORRELATION BETWEEN PLATEAU HEAT TRANSFER AND PLATEAU PRESSURE  
(REF. 10)







## Report Documentation Page

1. Report No.  NASA CR-4274		2. Government Accession No.		3. Recipient's Catalog No.	
4. Title and Subtitle  Flow Separation in Shock Wave Boundary Layer Interactions at Hypersonic Speeds				5. Report Date  February 1990	
				6. Performing Organization Code	
7. Author(s)  A. Hamed				8. Performing Organization Report No.	
				10. Work Unit No.  505-80-21-06	
9. Performing Organization Name and Address George Washington University Joint Institute for Advancement of Flight Sciences NASA Langley Research Center Hampton, VA 23665-5225				11. Contract or Grant No.  NAS1-18458, Task #19	
				13. Type of Report and Period Covered Contractor Report	
12. Sponsoring Agency Name and Address National Aeronautics and Space Administration Langley Research Center Hampton, VA 23665-5225				14. Sponsoring Agency Code	
15. Supplementary Notes  Langley Technical Monitor: Ajay Kumar Final Report  A. Hamed Department of Aerospace Engineering and Engineering Mechanics University of Cincinnati Cincinnati, OH 45221					
16. Abstract  This work presents an assessment of the experimental data on separated flow in shock wave turbulent boundary layer interactions at hypersonic and supersonic speeds. The data base consist mainly of two dimensional and axisymmetric interactions in compression corners or cylinder-flares, and externally generated oblique shock interactions with boundary layers over flat plates or cylindrical surfaces. The conditions leading to flow separation and the subsequent changes in the flow empirical correlations for incipient separation are reviewed. The effects of the Mach number, Reynolds number, surface cooling and the methods of detecting separation are discussed. The pertinent experimental data for the separated flow characteristics in separated turbulent boundary layer shock interaction are also presented and discussed.					
17. Key Words (Suggested by Author(s))  Hypersonic Flow Shock Wave Boundary Layer Interaction Flow Separation				18. Distribution Statement  Unclassified - Unlimited  Subject Category 02	
19. Security Classif. (of this report)  Unclassified		20. Security Classif. (of this page)  Unclassified		21. No. of pages  48	
				22. Price  A03	



